WYOMING STATE GEOLOGICAL SURVEY
Erin A. Campbell, Director and State Geologist
Laramie, Wyoming

Interpreting the past, providing for the future

OPEN FILE REPORT 2019-3
Garden Gulch 1:24,000-scale
Bedrock Geologic Map

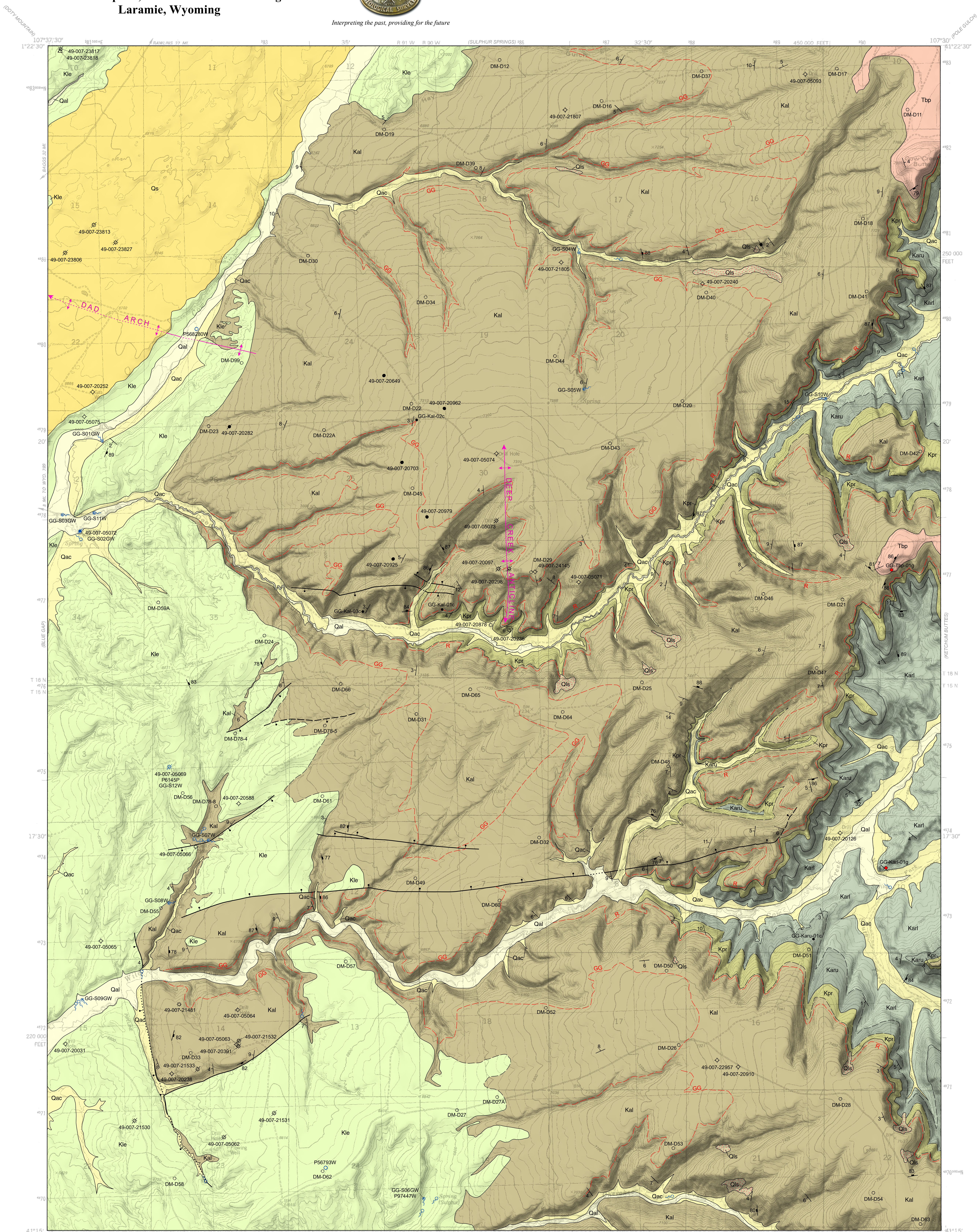

Base map from U.S. Geological Survey 1:24,000-scale topographic map of the Garden Gulch, Wyoming Quadrangle, 1982

Base hillshade derived from USDA/NRCS–National Geospatial Center of Excellence 10-meter Digital Elevation Model (DEM), 2000; azimuth 315º, sun angle 45º, vertical exaggeration 2.8

Projection: Universal Transverse Mercator (UTM), zone 13
North American Datum of 1927 (NAD 27)
1,000-meter grid ticks: UTM, zone 13
10,000-foot grid ticks: Wyoming State Plane Coordinate System, east central zone

Wyoming State Geological Survey
P.O. Box 1347 - Laramie, WY 82073-1347
Phone: 307-766-2286 - Fax: 307-766-2605
Email: wsgs-info@wyo.gov

MN
GN
1°42'
9°35'
UTM GRID AND 2019 MAGNETIC NORTH DECLINATION AT CENTER OF SHEET

SCALE 1:24,000

1 0.5 0 1 Mile

1,000 0 1,000 2,000 3,000 4,000 5,000 6,000 7,000 Feet

1 0.5 0 1 Kilometer

CONTOUR INTERVAL 20 FEET
NATIONAL GEODETIC VERTICAL DATUM OF 1929

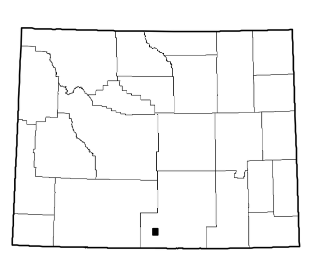

WYOMING QUADRANGLE LOCATION

Digital cartography by Ranie M. Lynds, Jesse R. Pisel, and Kara L. Hoppes

Map edited by Suzanne C. Luhr

Prepared in cooperation with and research supported by the U.S. Geological Survey, National Cooperative Geologic Mapping Program, under USGS award number G18AC00150. The views and conclusions contained in this document are those of the authors and should not be interpreted as necessarily representing the official policies, either expressed or implied, of the U.S. Government.

PRELIMINARY GEOLOGIC MAP OF THE GARDEN GULCH QUADRANGLE, CARBON COUNTY, WYOMING

by

Ranie M. Lynds, Jesse R. Pisel, Kara L. Hoppes, Karl G. Taboga, Seth J. Wittke, and Kelsey S. Kehoe

2019

EXPLANATION

CORRELATION OF MAP UNITS

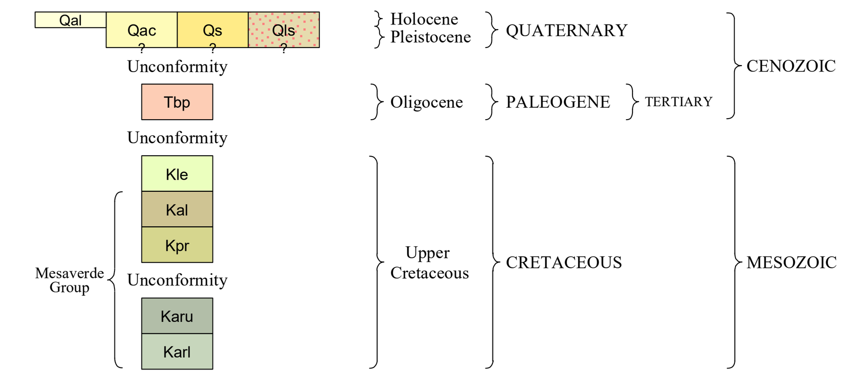

MAP SYMBOLS

Definitions: *Certain—Estimated location <25 m (82 ft)*
Approximate—Estimated location 25–100 m (82–330 ft)

Formation contact—Continuous where certain, long dash where approximate

Fault—Continuous where certain, long dash where approximate, dotted where concealed; bar and ball on downthrown block of normal fault

Anticline—Continuous where certain, dotted where concealed; arrow on end indicates direction of plunge

Coal bed—Modified from Dames & Moore (1979) and Haacke and others (2016). Abbreviations: Robertson coal (R); Garden Gulch coal (GG)

7 **Strike and dip of inclined bedding**

88 **Strike and dip of joint**

Strike of vertical joint

DM-D21 **Drill hole for coal exploration**—From Haacke and others (2016)

GG-Kal-03c **Coal quality sample**—Showing sample name; sampled for coal quality (c)

49-007-20649 **Oil well**—Showing API number

49-007-20910 **Oil well, plugged and abandoned**—Showing API number

49-007-05072, GG-S02GW **Oil well, plugged and abandoned, sampled**—Showing API number and sample name; sampled for gas (G) and water (W)

49-007-20878 **Gas well**—Showing API number

49-007-22957 **Gas well, plugged and abandoned**—Showing API number

49-007-05069, GG-S12W, P6145P **Gas well, plugged and abandoned, converted to water well, sampled**—Showing API number and sample name; sampled for water (W); includes water well permit number

49-007-05066 **Dry hole, plugged and abandoned**—Showing API number

49-007-23818 **Disposal well**—Showing API number

P568280W **Water well**—Showing permit number

Spring

GG-S08GW **Spring, sampled**—Showing sample name; sampled for gas (G) or water (W); includes water well permit number when appropriate

GG-Tbp-01g **Geochronology sample**—Showing sample name; sampled for geochronology (g)

DESCRIPTION OF MAP UNITS

Cenozoic

Qal **Alluvium (Holocene)**—Unconsolidated to poorly consolidated, subangular to subrounded clay, silt, sand, coarse gravels, and cobbles. Material locally derived. Thickness undetermined

Qac **Alluvium and colluvium (Holocene and Pleistocene[?])**—Unconsolidated to poorly consolidated, subangular to subrounded clay, silt, sand, gravels, and cobbles mixed with clay-rich soil; derived from local geologic units. Includes slope wash, debris flows, and alluvial fan deposits that coalesce with alluvium. Thickness less than 8 m (26 ft)

Qs **Sand (Holocene and Pleistocene[?])**—Unconsolidated sand dunes, silt, and clay; vegetation depends on degree of consolidation and active migration. Thickness less than 5 m (16 ft)

Qls **Landslide debris (Holocene and Pleistocene[?])**—Blocks and slumps of locally derived detritus from steep and unstable slopes. Most common at headwall of secondary drainages; often thickly vegetated. Width less than 300 m (980 ft) but frequently 150 m (490 ft); thickness less than 50 m (160 ft)

Tbp **Browns Park Formation (Oligocene)**—Light-gray to tan, calcareous to siliceous, medium- to coarse-grained sandstone, conglomerate, and rare accretionary limestone. Cross-bedded sandstone and conglomerate are poorly to moderately sorted, angular to sub-rounded, with clasts of chert, quartzite, and unidentified mafic and felsic igneous and metamorphic material. Outcrops are well indurated and distinguished by ferruginous yellowish-brown soil littered with white quartzite. Unconformably overlies all older formations. Although thickness can reach 760 m (2,500 ft) east in the Saratoga Valley (Montagne, 1991), only lowermost 45 m (150 ft) observed in map area. U-Pb detrital zircon geochronology (sample GG-Tbp-01g) from sandstone yields a maximum depositional age of 28.7 ± 0.3 Ma (weighted mean age at 2σ) at the base of the formation. Data table available in accompanying report

Mesozoic

Kle **Lewis Shale (Upper Cretaceous)**—Poorly exposed, gray to dark-gray, silty claystone and shale that is occasionally interbedded with burnt-orange and brown, very fine grained concretionary sandstones. Basal contact is distinct and conformable, mapped at the uppermost sandstone layer of the underlying Almond Formation. Thickness varies greatly in the region and can be more than 610 m (2,000 ft; Hettinger and others, 2008); only the basal 200 m (660 ft) occurs in the map area

Mesaverde Group (Upper Cretaceous)

Kal **Almond Formation**—Light- to medium-gray or beige, fine-grained sandstones interbedded with medium- to dark-gray fissile shale, carbonaceous shale, coal, and red to orange discontinuous beds of clinker. Sandstones are typically 1–3 m (3–10 ft) thick and crop out as resistant, symmetrically rippled, iron-stained and orange-weathering hilltops and dip slopes that are well exposed between nonresistant shale units. Two semi-continuous coal zones—the Robertson coal (R) near the base of the formation that commonly crops out as clinker and the Garden Gulch coal (GG) approximately 91 m (300 ft) above the base of the formation—were originally mapped by Haacke and others (2016). Basal contact is gradational and conformable. Approximately 125–151 m (410–495 ft) thick

Kpr **Pine Ridge Sandstone**—Light-gray to white, fine-grained, moderately resistant, cross-bedded sandstone interbedded with siltstone, claystone, organic shale, and coal. Weathers to blocky, light-gray, orange, or light-pink, iron-oxide-stained, massive outcrops that are often jointed and fractured. Rare iron-oxide boxwork fracture fill. Poorly exposed on north- to northwest-facing vegetated slopes where contact is approximate. Base is unconformable and sharp to gradational. Thickness less than 30 m (100 ft), commonly less than 9 m (30 ft)

Allen Ridge Formation

Karu **Upper member**—Nonresistant interbedded claystone, carbonaceous shale, coal, and rare lenticular sandstones. Claystone is brittle to fissile, dark gray, and locally carbonaceous. Sandstones are heavily bioturbated, carbonaceous, contain current and oscillation ripples, and weather tan to light red with slightly platy parting. Contrasts sharply with the well-exposed lower member of the Allen Ridge Formation and typically forms a steep slope beneath the more resistant Pine Ridge Sandstone. Lower contact is sharp and conformable. Approximately 30–43 m (100–140 ft) thick

Karl **Lower member**—Thick sequence of variegated orange-brown, tan, and light-gray, lenticular, very fine to fine-grained sandstones interbedded with shale, carbonaceous shale, coal, and concretionary sandstone lenses. Sandstones are generally cross-bedded and commonly bioturbated with frequent rip-up clasts, soft-sediment deformation, flaser bedding, current ripples, trace fossils, and root traces. Weathers to blocky sandstone. Well exposed in the eastern drainage of Wild Cow Creek, where sandstone sample GG-Karl-01g was collected for U-Pb geochronology; data table available in accompanying report. Basal contact is sharp and conformable but not exposed; uppermost 122 m (400 ft) exposed in map area

TYPE LOG

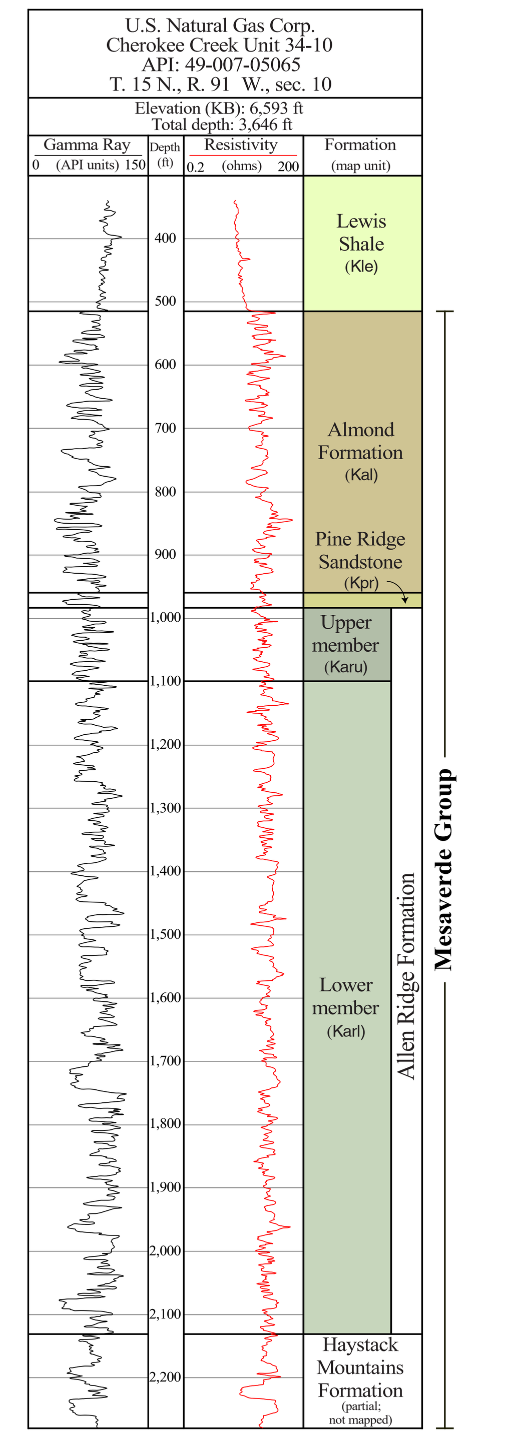

REFERENCES

Barclay, C.S.V., 1980a, Geophysical logs and coal sections of holes drilled during 1977 and 1978 in T. 15 N., Rs. 90 and 91 W., Ketchum Buttes and Doty Mountain quadrangles, Carbon County, Wyoming: U.S. Geological Survey Open-File Report 80-488, 16 p., 115 pls.

Barclay, C.S.V., 1980b, Geophysical logs and coal sections of holes drilled during 1977 and 1978 in T. 16 N., Rs. 90 and 91 W., Ketchum Buttes and Doty Mountain quadrangles, Carbon County, Wyoming: U.S. Geological Survey Open-File Report 80-643, 10 p., 122 pls.

Barclay, C.S.V., and Shoaff, L.A., 1977, Lithologic and geophysical logs of holes drilled in the Doty Mountain, Browns Hill, and Baggs quadrangles, Carbon County, Wyoming, during 1976: U.S. Geological Survey Open-File Report 77-171, 77 p., 65 pls.

Barclay, C.S.V., and Zimmermann, S.C., 1976, Lithologic and geophysical logs of holes drilled in the eastern part of the Doty Mountain quadrangle, Carbon County, Wyoming, by the U.S. Geological Survey during 1975: U.S. Geological Survey Open-File Report 76-510, 108 p., 41 pls.

Dames & Moore, 1979, Coal resource occurrence and coal development potential maps of the SE quarter of the Doty Mountain 15-minute quadrangle, Carbon County, Wyoming: U.S. Geological Survey Open-File Report 79-1032, 28 p., 28 pls., scale 1:24,000.

Gill, J.R., Merewether, E.A., and Cobban, W.A., 1970, Stratigraphy and nomenclature of some Upper Cretaceous and lower Tertiary rocks in south-central Wyoming: U.S. Geological Survey Professional Paper 667, 53 p.

Haacke, J.E., Barclay, C.S.V., and Hettinger, R.D., 2016, Preliminary geologic mapping of Cretaceous and Tertiary formations in the eastern part of the Little Snake River coal field, Carbon County, Wyoming: U.S. Geological Survey Open-File Report 2016-1170, 9 p.

Hettinger, R.D., and Honey, J.G., 2005, Geologic map and coal stratigraphy of the Blue Gap quadrangle, eastern Washakie Basin, Carbon County, Wyoming: U.S. Geological Survey Scientific Investigations Map 2878, 2 sheets, scale 1:24,000.

Hettinger, R.D., Honey, J.G., Ellis, M.S., Barclay, C.S.V., and East, J.A., 2008, Geologic map of Upper Cretaceous and Tertiary strata and coal stratigraphy of the Paleocene Fort Union Formation, Rawlins-Little Snake River area, south-central Wyoming: U.S. Geological Survey Scientific Investigations Map 3053, 3 sheets, scale 1:100,000.

Montagne, John, 1991, Cenozoic history of the Saratoga Valley area, Wyoming and Colorado: Contributions to Geology, v. 29, no. 1, p. 13–70, 4 pls.

Roehler, H.W., 1990, Stratigraphy of the Mesaverde Group in the central and eastern Greater Green River Basin, Wyoming, Colorado, and Utah: U.S. Geological Survey Professional Paper 1508, 52 p., 2 pls.

Scott, J.E., Sutherland, W.M., Johnson, Joe, and McLaughlin, J.F., 2011, Geologic map of the Baggs 30’ x 60’ quadrangle, Carbon and Sweetwater counties, Wyoming, and Moffat and Routt Counties, colorado: Wyoming State Geological Survey Map Series 95, 33 p., scale 1:100,000.

WOGCC, 2018, Wyoming Oil and Gas Conservation Commission, accessed May 2018, at http://wogcc.state.wy.us/.

WSEO, 2018, Wyoming State Engineer’s Office, accessed November 2018, at https://sites.google.com/a/wyo.gov/seo/.

Interpreting the past, providing for the future

Preliminary Geologic Map of the Garden Gulch 7.5' Quadrangle, Carbon County, Wyoming

By Ranie M. Lynds, Jesse R. Pisel, Kara L. Hoppes, Karl G. Taboga, Seth J. Wittke, and Kelsey S. Kehoe

Open File Report 2019-3
June 2019

Wyoming State Geological Survey

Erin A. Campbell, Director and State Geologist

Preliminary Geologic Map of the Garden Gulch 7.5’ Quadrangle, Carbon County, Wyoming

By Ranie M. Lynds, Jesse R. Pisel, Kara L. Hoppes, Karl G. Taboga, Seth J. Wittke, and Kelsey S. Kehoe

Layout by Christina D. George

Open File Report 2019-3
Wyoming State Geological Survey
Laramie, Wyoming: 2019

This Wyoming State Geological Survey (WSGS) Open File Report is preliminary and may require additional compilation and analysis. Additional data and review may be provided in subsequent years. For more information about the WSGS, or to download a copy of this Open File Report, visit www.wsgs.wyo.gov. The WSGS welcomes any comments and suggestions on this research. Please contact the WSGS at 307-766-2286, or email wsgs-info@wyo.gov.

Citation: Lynds, R.M., Pisel, J.R., Hoppes, K.L., Taboga, K.G., Wittke, S.J., and Kehoe, K.S., 2019, Preliminary geologic map of the Garden Gulch 7.5’ quadrangle, Carbon County, Wyoming: Wyoming State Geological Survey Open File Report 2019-3, 25 p., scale 1:24,000.

Table of Contents

List of Figures

List of Tables

List of Tables in the Appendices

INTRODUCTION

The Garden Gulch 1:24,000-scale quadrangle is located in south-central Wyoming (fig. 1) on the eastern margin of the Washakie Basin, also known as the Atlantic Rim. The Upper Cretaceous and Paleogene strata along the Atlantic Rim dip westward toward the basin, gently folded by the west-plunging Dad Arch. The Garden Gulch quadrangle is on the eastern crest of the Dad Arch. Within the quadrangle, Oligocene conglomerates unconformably overlie middle Campanian to lower Maastrichtian (Upper Cretaceous) strata.

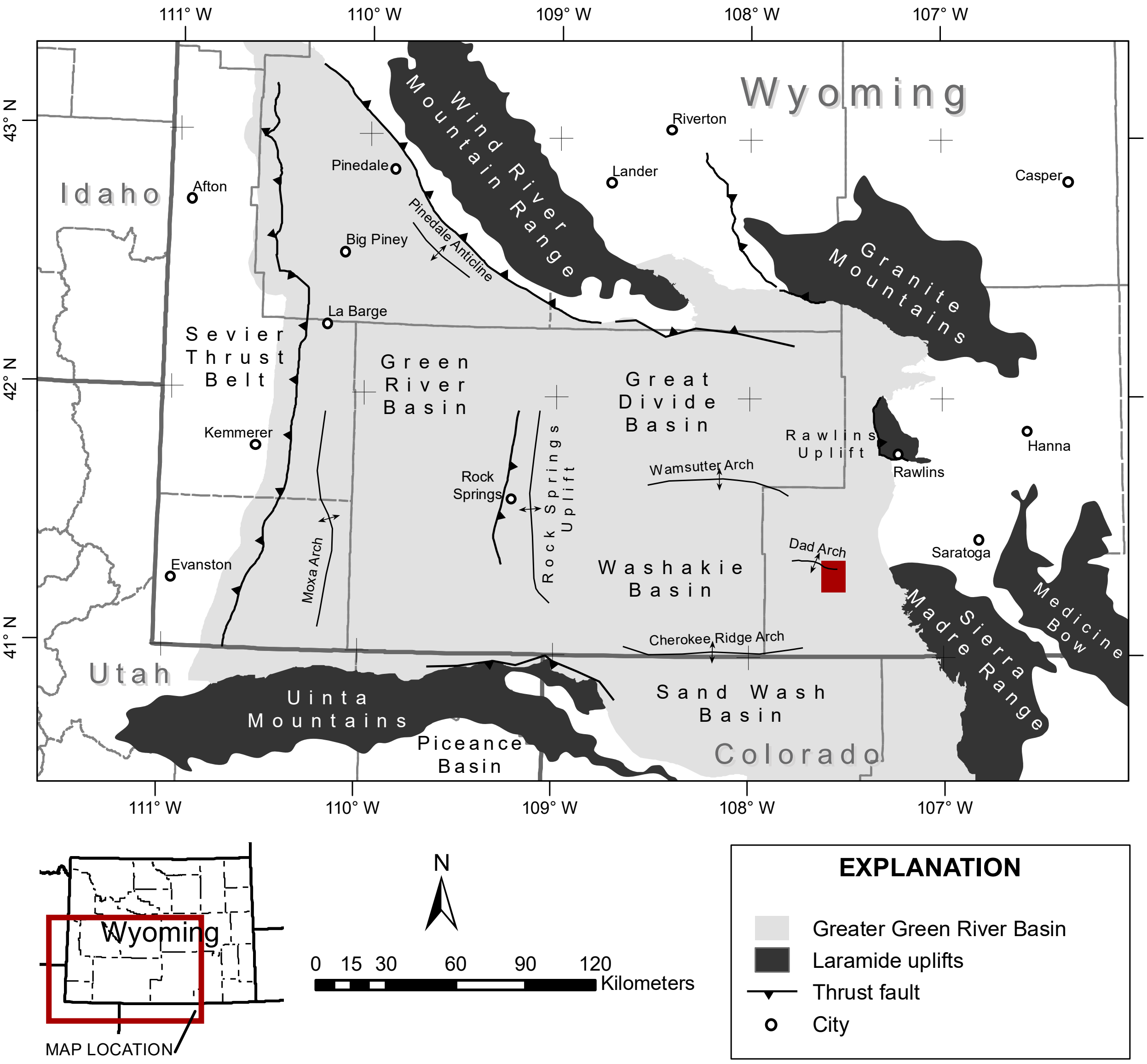

Figure 1. Map showing location of the study area in the Greater Green River Basin of south-central Wyoming. Extent of the Garden Gulch quadrangle is shown as a solid red rectangle. Counties are outlined as gray lines. Major structural features, sub-basins, and surrounding uplifts are noted.

Hettinger and others (2008) completed the first modern geologic map of the Atlantic Rim at the scale of 1:100,000, followed by Scott and others' (2011) geologic map of the Baggs 1:100,000-scale quadrangle. Much of Hettinger and others' (2008) work was based on unpublished 1:24,000-scale mapping by V.S. Barclay of the U.S. Geological Survey (USGS), later published as georeferenced field-copy maps by Haacke and others (2016). Adjacent 1:24,000-scale maps to the northwest, west, and southwest include the Doty Mountain (Hettinger and Honey, 2006), Blue Gap (Hettinger and Honey, 2005), and Peach Orchard Flat (Honey and Hettinger, 2004) quadrangles, respectively.

In addition to geologic mapping of the Garden Gulch quadrangle, this study collected coal-quality and geochronology data. Numerous natural springs and two wells (originally drilled as oil and gas exploration wells) were sampled for water quality. One well and several of these springs are point-source emitters of natural gas; gas samples were collected and analyzed for composition and carbon and hydrogen isotopes.

Field mapping and sample collection occurred during June through October 2018. Field data were integrated with satellite imagery interpretation as well as previous mapping and descriptions. The results were completed in cooperation with USGS 2018 StateMap grant award G18AC00150.

Location

The Washakie Basin covers approximately 4,800 km^2 (3,000 mi^2) of the southeastern part of the Greater Green River Basin, and is bounded by the Rock Springs Uplift to the west, the Wamsutter Arch to the north, the Sierra Madre Range to the east, and the Cherokee Ridge Arch to the south (Roehler, 1992). The Garden Gulch 7.5' quadrangle (Tps. 15–16 N. and Rgs. 90–91 W.), located in Carbon County, Wyoming, is situated on the eastern margin of the Washakie Basin (fig. 1).

The southern edge of the quadrangle is approximately 24 km (15 mi) north of Baggs, Wyoming. Nearly all of the land within the quadrangle is public and easily accessible via County Road 608 (Wild Cow Road) east from its junction with Wyoming Highway 789. Other roads that access the map area include Bureau of Land Management (BLM) Road 3305 (Willows Road), which branches off County Road 608 to intersect the northwestern corner of the quadrangle, and BLM Road 3308 (J O Road), which branches off from BLM Road 3305 and transects the map area parallel to the northern rim of Deep Gulch. Many other two-track roads exist within the quadrangle as well.

Cow Creek Butte is a prominent feature within the Garden Gulch quadrangle. Cow Creek Butte is a topographic high located about 1 km (0.6 mi) south of the northeast corner of the quadrangle. Resistant carbonate-cemented limestone and sandstone of the Oligocene Browns Park Formation cap the butte.

To the west of Cow Creek Butte lies Cow Creek, Garden Gulch, and numerous east–west-oriented ephemeral streams. Cutting through the center of the quadrangle is Deep Gulch and the southern branch of Cow Creek. The J O Ranch Rural Historic Landscape is located 1.6 km (1 mi) from where the northern branch of Cow Creek exits the western margin of the map. In the southern third of the quadrangle, Wild Cow Creek and several of its tributaries flow from the northeast to southwest. Cherokee Creek is the southern-most drainage in the map area, covering approximately 3 km (1.9 mi) of the southeastern margin of the map. Additionally, there are numerous springs that range from stagnant ground seeps to bubbling pools that expel both natural gas and flowing water. These springs are spread across the western half of the quadrangle, commonly located in either the Lewis Shale or Almond Formation.

GEOLOGY

Upper Cretaceous sedimentary rocks of the Mesaverde Group and Lewis Shale compose most of the outcrops within the Garden Gulch 7.5' quadrangle. Crustal loading associated with the Sevier orogeny to the west provided accommodation for the Mesaverde Group and Lewis Shale in the form of the Western Interior Foreland Basin (Steidtmann, 1993; Luo, 2005). During the Late Cretaceous, high global sea levels flooded the Western Interior Foreland Basin, forming the Western Interior Seaway. The Western Interior Seaway was a broad epicontinental sea spanning western North America, connecting the Arctic Ocean and Gulf of Mexico (Slattery and others, 2015), and covering most of Wyoming during this time, including much of the Washakie Basin. During the Late Cretaceous, rivers transported sediment from west to east toward the Western Interior Seaway. The Upper Cretaceous sedimentary rocks within the map area are the result of sediment deposition from these rivers, both at and near the coastline (Martinsen and others, 1999; Gomez-Veroiza and Steel, 2010). Local to regional variations in depositional patterns from the Upper Cretaceous through Eocene strata suggest onset of the Laramide orogeny and asynchronous uplift of the basin-bounding mountain ranges (Pasternak, 2005; Bader, 2008).

The oldest Upper Cretaceous unit exposed in the quadrangle, the middle Campanian Allen Ridge Formation (fig. 2), records the end of the second-to-last transgression of the Western Interior Seaway, or the Claggett transgression (Slattery and others, 2015). The Allen Ridge Formation documents sea level rise, as the fluvial facies of the lower member transition to paludal and estuarine facies of the upper member. Although the upper member of the Allen Ridge Formation has previously been described as marine in origin—it is termed the "marine member" by Merewether (1971)—observations of coal and shallow sandy channel forms suggest a terrestrial origin at some locations, at least within the map area. For these reasons, we map the Allen Ridge Formation with a lower and upper member instead of a main body (lower) and marine member (upper). U-Pb detrital zircon geochronology for a sample collected near the base of the lower member of the Allen Ridge Formation yields a maximum depositional age of 76.92 ± 1.03 Ma (weighted mean age at 95 percent confidence; Appendix 1).

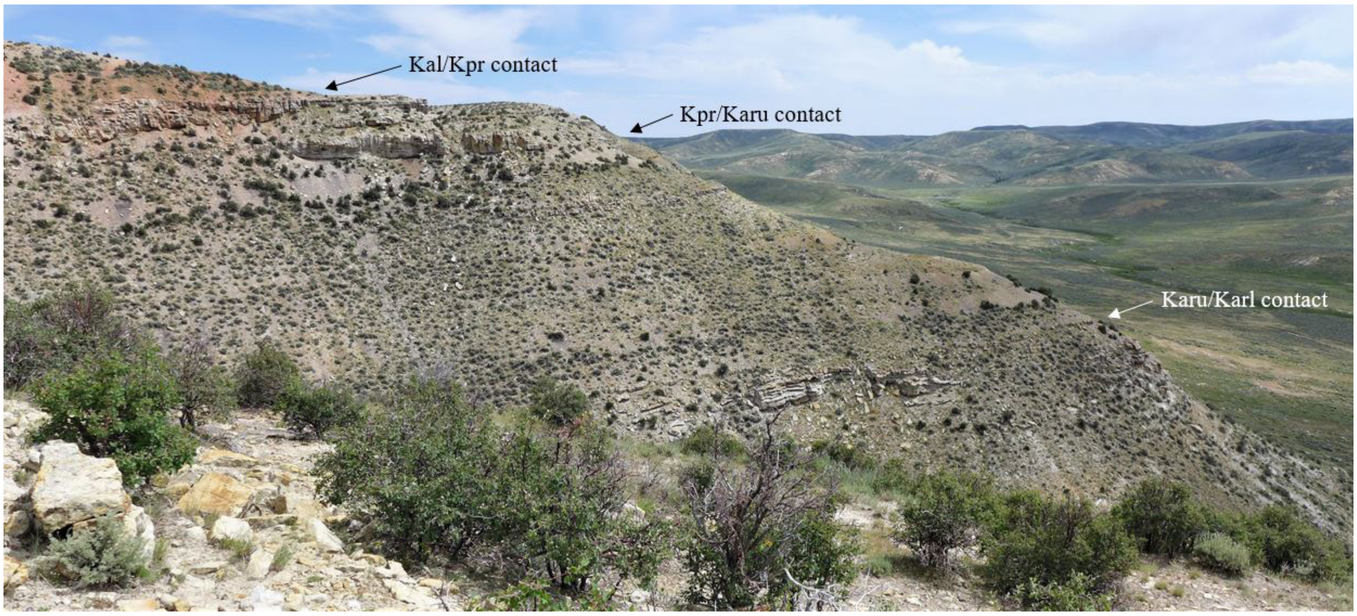

Figure 2. Photograph of contacts between the Almond Formation (Kal), the underlying Pine Ridge Sandstone (Kpr), and both the upper and lower members of the Allen Ridge Formation (Karu, Karl). The upper member of the Allen Ridge Formation shows a characteristic slope break at the contact with the more resistant Pine Ridge Sandstone.

Following the Claggett transgression was a period of sea level regression and uplift of the Moxa Arch on the western side of the Greater Green River Basin, resulting in erosion and an unconformity at the top of the Allen Ridge Formation. During the regression, rivers moved eastward across the quadrangle and deposited the sediments of the fluvial (upper Campanian) Pine Ridge Sandstone (figs. 2 and 3; Gill and Cobban, 1966; Reynolds, 1967).

Post-deposition of the Pine Ridge Sandstone, sea level rise and increased accommodation in the basin initiated the Bearpaw transgression (Gill and Cobban 1966; Gill and others 1970; Slattery and others 2015), the last major transgression by the Western Interior Seaway.

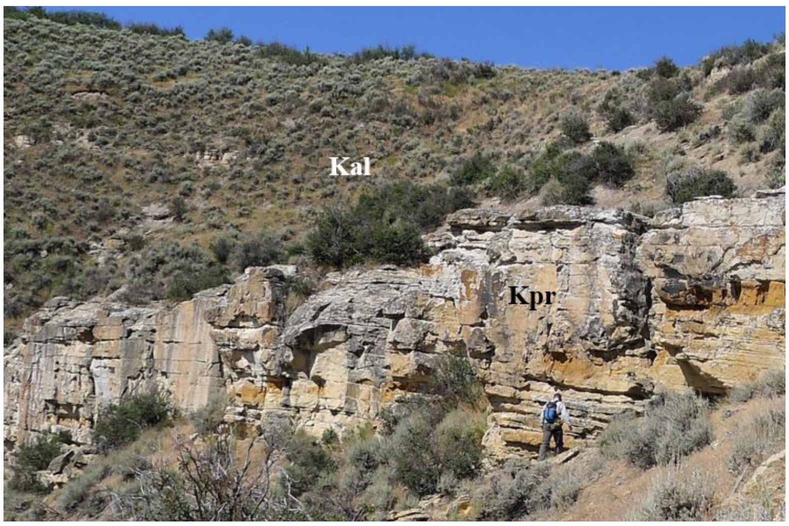

Figure 3. Photograph of an outcrop of the Pine Ridge Sandstone (Kpr) overlain by the Almond Formation (Kal) west of the South Fork of Wild Cow Creek. View is to the southwest, geologist for scale is 1.8 m (6 ft) tall.

During the Bearpaw transgression, rivers deposited the fluvial facies and coals (fig. 4) of the upper Campanian Almond Formation in a coastal plain to shallow marine setting. Transgression continued, leaving behind the marine Lewis Shale (Gill and others, 1970; Roehler, 1990; Kauffman and Caldwell, 1993; Steidtmann, 1993; Luo, 2005; Luo and Nummedal, 2010). The Maastrichtian Fox Hills Sandstone, Lance Formation, and Paleocene Fort Union Formation record the final regression of the Western Interior Seaway and are exposed on the adjacent Blue Gap quadrangle (Hettinger and Honey, 2005) to the west of the Garden Gulch quadrangle.

Figure 4. Photograph of a coal bed at the top of the Almond Formation. The geologist is pointing to the contact between the Almond Formation and the overlying Lewis Shale.

Through much of the Paleogene, the Laramide orogeny continued to segment the Western Interior Foreland Basin into smaller basins by Precambrian-cored uplifts. The formations deposited in many of these basins from the Paleocene through lower Oligocene are not preserved in the map area. However, the upper Oligocene Browns Park Formation, exposed on Cow Creek Butte (fig. 5) and an unnamed high point on the eastern part of the map area, documents Paleogene basin filling driven by erosion of the Sierra Madre uplift to the east (Montagne, 1991). Considered to be the product of fluvial, alluvial, and paludal processes, the Browns Park Formation thickens dramatically to the east into the Saratoga Valley, where the base was dated at 23.044 ± 0.154 Ma (Ar^{40}/Ar^{39} on biotite; Montagne, 1991). In the type section of the Browns Park Formation in Moffat County, Colorado, Izett and others (1970) record a K-Ar age of 24.8 ± 0.8 Ma at the base of the formation. U-Pb detrital zircon geochronology conducted as part of this study yields a maximum depositional age at the base of the formation of 28.69 ± 0.21 Ma (weighted mean age at 95 percent confidence; Appendix 1), coincident with the end of the Bishop Conglomerate fluvial system in the central Greater Green River Basin to the west (Aslan and others, 2017). More work is required to document the stratigraphic and geochronologic relationship within the Browns Park Formation, as well as its association with the coeval Bishop Conglomerate.

Figure 5. Photograph of the highly silicified sandstone outcrop of the Browns Park Formation on Cow Creek Butte. Hammer in photograph is 20 cm (7.9 in) long.

During the Holocene and possibly the later Pleistocene, alluvial and eolian processes eroded the strata within the Garden Gulch quadrangle, forming alluvium, colluvium (fig. 6), and windblown sand (fig. 7). Windblown deposits are especially prevalent as a dune field in the northwest corner of the map, near the J O Ranch. Active parabolic dunes exist to the north of the map within the same dune field. Landslides in the mapped area are primarily confined to the drainage rims (fig. 8). Block-slide-type failure make up the majority of landslides, originating from sandstone units in the Almond Formation. Rock fall has also occurred in steeper drainages along Wild Cow Creek and Deep Gulch.

Figure 6. Photograph of mixed alluvium and colluvium in the Cherokee Creek drainage. Escarpment approximately 3 m (10 ft) high.

Structure

Regional westward dip in the Garden Gulch 7.5' quadrangle is shallow, generally much less than 10°. The gentle dip is due to the west-plunging Dad Arch anticlinal axis that crosses the northern margin of the map area (Hettinger and others, 2008). Local variations in bedding inclination near the center of the map highlight the north–south-trending, doubly plunging Deep Creek Anticline (Dames & Moore, 1979).

Normal faults along the Atlantic Rim are oriented northeast to southwest, while reverse faults along the rim are oriented northwest to southeast (Hettinger and Honey, 2005). Faults along the southern margin of the Washakie Basin associated with the Cherokee Ridge Arch are high-angle normal faults that cut through Upper Cretaceous through Oligocene and possibly Miocene strata. The Cherokee Ridge Arch (fig. 1) is the result of periodic left-lateral

Figure 7. Photograph of densely vegetated sand dunes in the northwest corner of the map area.

Figure 8. Photograph showing a characteristic north-facing landslide. The landslide is in the center of the photograph covered with green vegetation.

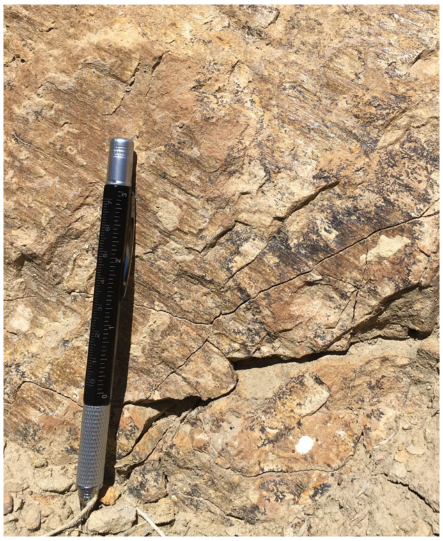

Figure 9. Photograph of slickensides in the Almond Formation located along a fault trace on the north side of Deep Gulch. Scale on the left half of the pen is incremented in centimeters.

strike-slip movement beginning in the Late Cretaceous and continuing through the Miocene (Bader, 2008). During the Paleogene and Neogene, the Atlantic Rim and Washakie Basin underwent extension, which provided vertical accommodation space for the Browns Park Formation (Bader, 2008).

Although the structure observed in the Garden Gulch area is not complex, evidence of syndepositional faulting in the Almond Formation elsewhere in the Greater Green River Basin suggests episodic movement of the Rock Springs Uplift and Wamsutter Arch (Barlow, 1961). In the map area, Haacke and others (2016) identified and mapped several normal faults. Observed in the field, slickensides (fig. 9) rarely accompany these normal faults. Vertical offset from these faults does not exceed 2.5 m (8 ft).

In the map area, we collected 185 joint measurements from the Cretaceous and Oligocene units (fig. 10). The joint sets are numbered 1 through 4, with J1 corresponding to the first group, J2 the second group, and so on. The J1 and J2 fracture sets have similar north-south orientations, as the J1 fracture set has a mean azimuth of 185° and dip of 83° (n=71), and the J2 fracture set has a mean azimuth of 007°and dip of 82° (n=51). The J3 and J4 fracture sets have an east-west orientation. The J3 fracture set has a mean azimuth of 276° and dip of 81° (n=29), and the J4 fracture set has an azimuth of 102° and dip of 70° (n=34).

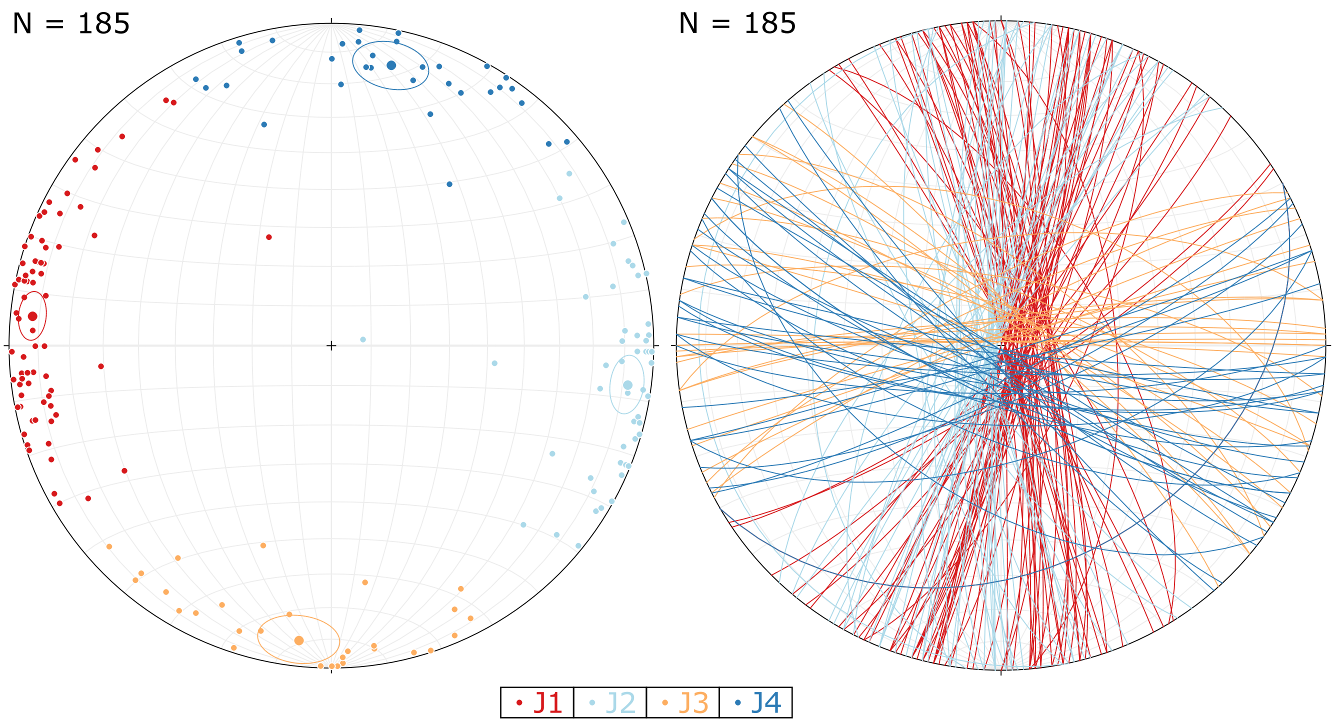

Figure 10. Equal area stereonet plots of joint measurements in the Garden Gulch quadrangle. On the left are the normal to the joint planes, with mean vectors represented by larger points and the standard deviation represented by the circle around the larger point. On the right is the equal area stereonet plot of the joint planes; both plots are colored by the fracture sets J1–J4.

ECONOMICS

Oil and Natural Gas

Exploration for oil and natural gas in the Garden Gulch quadrangle began in 1917. Forty-four wells have been drilled to date, with production from 18 natural gas wells and 6 oil wells (WOGCC, 2019; table 1). While all of the oil wells are currently producing, only two of the natural gas wells remain productive. Combined, from 1978 through 2018, the wells in the map area produced 2.99 billion cubic feet of natural gas, 190,405 barrels of oil, and 9.03 million barrels of water (WOGCC, 2019). Drilling targets include Upper Cretaceous coals and sandstones of the Mesaverde Group, as well as the deeper Upper Cretaceous Shannon and Sussex sandstones.

To confirm the location and status of wells within the map area, wells and abandoned well sites were physically located in the field. We recorded the position of all ground locations with handheld GPS and noted the well status. Any additional information available at the well site, such as well name, lease number, and company, were also documented and used to compare with WOGCC (2019) records.

Table 1. Field-verified locations and status for wells within the quadrangle (WOGCC, 2019).

API Number	Well Name	Company	Latitude (NAD27)	Longitude (NAD27)	Year	Status	Total Depth (ft)	Gas Produced (Mcf)	Oil Produced (Bbl)	Water Produced (Bbl)	Producing or Target Formation
49-007-05062	FEDERAL 32-23	Warren E & P INC	41.25983	-107.60032	1964	PA	11,246	541,487	442	317	FRONTIER/STEELE
49-007-05063	FEDERAL 14-1	Decalta International Corp	41.26963	-107.59856	1959	DH	2,725	-	-	-	DEEP CREEK
49-007-05064	FEDERAL 1	Vaughn JR GH	41.27327	-107.59837	1957	DH	2,730	-	-	-	UNKNOWN
49-007-05065	UNIT 34-10	US Natural Gas Corp	41.28054	-107.61752	1964	DH	3,646	-	-	-	UNKNOWN
49-007-05066	FEDERAL 11-3	Griffin Bennie C	41.29048	-107.60426	1991	DH	10,500	-	-	-	UNKNOWN
49-007-05069	UNIT 13-2	McCulloch Oil	41.29890	-107.60795	1954	PA	9,129	-	-	-	FRONTIER
49-007-05071	UNIT 2	Amerada Hess Corporation	41.31841	-107.55067	1950	DH	2,527	-	-	-	MESAVERDE
49-007-05072	GOVT 1	New Era Oil/Preferred Energy	41.32390	-107.62047	1954	DH	800	-	-	-	UNKNOWN
49-007-05073	DEEP CREEK UNIT 1	Amerada Hess Corporation	41.32492	-107.56220	1950	PA	8,275	-	-	-	MESAVERDE
49-007-05074	DEEP CREEK UNIT 1	Explorations INC	41.33198	-107.56216	1960	DH	3,400	-	-	-	UNKNOWN
49-007-05075	CH 058476 1	Hughes Oil Company INC	41.33587	-107.61990	1917	DH	400	-	-	-	UNKNOWN
49-007-05093	GOVT-SAYLER 1	CHS McPherson Refinery INC	41.37200	-107.51891	1958	DH	2,628	-	-	-	UNKNOWN
49-007-20031	FED-CHEROKEE CREEK 23-15	US Natural Gas Corp	41.26966	-107.62247	1967	DH	3,145	-	-	-	UNKNOWN
49-007-20097	FEDERAL 31-31	True Oil LLC	41.31983	-107.56192	1970	PA	10,191	-	-	-	DEEP CREEK
49-007-20126	FEDERAL 4-10	Kissinger Petroleum Corp	41.29192	-107.51410	1971	DH	7,274	-	-	-	UNKNOWN
49-007-20236	BROWNS HILL J-31	Golden Oilfield Operations INC	41.31334	-107.56041	1975	PA	7,045	126,908	85	23	DEEP CREEK
49-007-20238	CHEROKEE CREEK 13-14	Exeter Drilling Company	41.26653	-107.60758	1975	DH	8,525	-	-	-	UNKNOWN
49-007-20240	ISABELLE FEDERAL 1	Davis Oil Company	41.34988	-107.53333	1975	DH	7,719	-	-	-	UNKNOWN
49-007-20252	DEEP GULCH UNIT 1	Home Petroleum Corporation	41.33845	-107.61873	1976	DH	8,784	-	-	-	FRONTIER
49-007-20282	CHEROKEE CREEK B-26	Benson-Montin-Greer Drilling Corp	41.33481	-107.59957	1989	PA	8,496	1,115	223	1,210	SHANNON
49-007-20298	BROWNS HILL UNIT B-31	Benson-Montin-Greer Drilling Corp	41.31985	-107.56041	1976	PA	2,434	529,517	-	6,152	DEEP CREEK
49-007-20391	FEDERAL Y 1	TXO Production Corporation	41.26945	-107.59827	1979	PA	8,500	140,098	929	340	FRONTIER
49-007-20588	FEDERAL 3654 15-2	Anschutz Corporation	41.29504	-107.59827	1980	DH	2,845	-	-	-	UNKNOWN
49-007-20649	CHEROKEE CRK FED 24-1	Golden Oilfield Operations INC	41.34023	-107.57791	1981	SI	7,720	28,207	43,984	1,479	SHANNON
49-007-20703	CHEROKEE CRK FED 25-5	Golden Oilfield Operations INC	41.33105	-107.57539	1981	SI	4,500	33,133	61,511	429	SHANNON
49-007-20878	BROWN'S HILL J-31-X	Golden Oilfield Operations INC	41.31388	-107.56294	1982	SI	7,638	100,975	2,409	60,235	FRONTIER
49-007-20910	CHEVRON-STATE 1-16	Chevron USA INC	41.26727	-107.52838	1983	DH	5,100	-	-	-	UNKNOWN
49-007-20925	CHEROKEE CREEK A36	Julander Energy Company	41.32087	-107.57663	1983	SI	4,721	40,839	21,706	4,546	SHANNON
49-007-20962	CHEROKEE CREEK UNIT D-30	Golden Oilfield Operations INC	41.33676	-107.56947	1983	SI	4,513	47,247	20,848	3,140	SHANNON
49-007-20979	CHEROKEE CREEK UNIT M-30	Golden Oilfield Operations INC	41.32531	-107.57189	1984	SI	4,488	113,167	9,312	2,518	SHANNON
49-007-21481	FEDERAL 1-5-14	Warren E & P INC	41.27385	-107.60654	1995	SI	7,761	312,843	23,597	11,005	NIOBRARA/SUSSEX
49-007-21530	WILD COW CREEK UNIT 1-22	Warren E & P INC	41.26157	-107.61280	1996	PA	7,807	-	-	-	SUSSEX
49-007-21531	WILD COW CREEK 1-23	Warren E & P INC	41.26238	-107.59328	1996	PA	4,662	21,224	257	458	COW CREEK
49-007-21532	WILD COW CREEK 10-14	Warren E & P INC	41.27001	-107.59821	1996	PA	4,720	330,329	1,366	20,076	COW CREEK
49-007-21533	WILD COW CREEK 14-14	Warren E & P INC	41.26703	-107.60398	1996	PA	8,500	290,833	3,736	66,645	MUDDY/DAKOTA
49-007-21805	PITT & MIDWAY 1690 13-17	Warren E & P INC	41.35215	-107.55312	2000	DH	473	-	-	-	MESAVERDE
49-007-21807	DAD-SULPHUR P8-1	Warren E & P INC	41.36824	-107.55257	1999	DH	567	-	-	-	ALMOND (COAL)
49-007-22957	STATE 2-16	Redwine Resources INC	41.26796	-107.53133	2006	DH	1,100	-	-	-	MESAVERDE (COAL)
49-007-23806	SUN DOG UNIT 1691 14-15	Warren E & P INC	41.35314	-107.62259	2008	PA	1,446	154,015	-	1,783,157	MESAVERDE (COAL)
49-007-23813	SUN DOG UNIT 1691 10-15	Warren E & P INC	41.35610	-107.61857	2008	PA	1,405	73,053	-	1,925,179	PINE RIDGE
49-007-23817	SUN DOG UNIT 1691 6-10 AR	Warren E & P INC	41.37465	-107.62325	2009	PA	1,860	50,072	-	3,725,617	MESAVERDE (COAL)
49-007-23818	SUN DOG UNIT 1691 6-10I AR	Warren E & P INC	41.37443	-107.62328	2009	AI	3,699	-	-	-	MESAVERDE (COAL)
49-007-23827	SUN DOG UNIT 1691 16-15	Warren E & P INC	41.35425	-107.61552	2008	SI	1,380	61,738	-	1,421,118	PINE RIDGE
49-007-24145	DEEP CREEK FIELD 4-2-31	Golden Oilfield Operations INC	41.31950	-107.55680	2010	DH	2,600	-	-	-	DEEP CREEK

Coal

Coal-bearing units in the Garden Gulch quadrangle are the Allen Ridge, Pine Ridge, and Almond formations. Coal has not been mined in the map area. The coals in the Almond Formation along the Atlantic Rim are subbituminous A, while coals from the Allen Ridge Formation are high-volatile C bituminous (Dames & Moore; 1979). Coal quality from four outcrop samples is reported in Appendix 2.

In the Almond Formation, Dames & Moore (1979) recognize nine mapped coal beds or zones: Robertson 1 and 2, Almond 1 and 2, Almond local 1–4, and Garden Gulch. Dames & Moore (1979) calculated coal reserve base tonnages within the Garden Gulch quadrangle for areas of high, moderate, and low development potential. The reserve base for strippable potential coal is as follows: high development potential coal is 56.77 million metric tons (62.58 million short tons), moderate development potential coal is 54.26 million metric tons (59.81 million short tons), and low development potential coal is 87.84 million metric tons (96.83 million short tons). Total reserve base is highest for the Almond 2 coal bed at 53.66 million metric tons (59.16 million short tons), followed by the Robertson coal bed at 48.56 million metric tons (53.53 million short tons), the Garden Gulch coal bed at 44.83 million metric tons (49.42 million short tons), and the Almond 2 coal bed at 42.48 million metric tons (46.83 million short tons). The remaining five coal beds have a total combined reserve base of 9.326 million metric tons (10.28 million short tons).

Uranium

There are no historical or active uranium mines in the Garden Gulch quadrangle. However, there are inactive uranium prospect pits and reclaimed open pit mines in the adjacent Ketchum Buttes and Browns Hill quadrangles to the east and southeast, respectively. These prospects targeted the upper 20 m (66 ft) of the Browns Park Formation where uranium is concentrated in limestone and sandstone (Wilson, 2015; Carroll and others, 2016). On the Browns Hill quadrangle there are two unnamed prospect pits located in secs. 26 and 35, T. 15 N., R. 90 W. The Ketchum Buttes quadrangle has six inactive prospect pits in the southeast quarter of the quadrangle named the Ketchum Buttes Uranium Area (Wilson, 2015). The uranium pay zone is located in the upper portion of the Browns Park Formation. Uranium potential is low in the study area as only the basal Browns Park Formation is preserved on the Garden Gulch quadrangle.

Industrial Materials

The Garden Gulch quadrangle has no known deposits of industrial minerals, however, potential silica and aggregate sources are summarized below.

Silica

The sand dunes in the northwest corner of the quadrangle are a potential source of silica. Further investigation would be needed to determine the suitability of this sand for industrial purposes, including grain size, sorting, rounding, crushability, and silica content.

Aggregate

Alluvial gravels are not common in the quadrangle, yet there is potential for development of aggregate materials from the Browns Park Formation. There are two active aggregate pits mining rock from the Browns Park Formation located 5 km (3 mi) south of the map area in secs. 2 and 11, T. 14 N., R. 90 W. (Sutherland and others, 2018).

HYDROLOGY

Surface Hydrology

Four alluvial streams flow from east to west through the Garden Gulch quadrangle. These are named, from north to south, Cow Creek, Deep Gulch, Wild Cow Creek, and Cherokee Creek, and are shown as perennial streams on the USGS topographic map. These four streams discharge to Muddy Creek about 6 km (3.75 mi) to the southwest of the Garden Gulch quadrangle. Deep Gulch and Garden Gulch are tributaries to Cow Creek, the northern-most perennial stream that flows across the northwest corner of the quadrangle.

Stream gradients vary from 20 m/305 m (66 ft/1,000 ft) in the highest reaches of Garden Gulch to 1.5 m/305 m (5 ft/1,000 ft) in Wild Cow Creek on the western edge of the quadrangle. Stream sinuosity in Cow Creek, Deep Gulch, and Wild Cow Creek range from less than 1.2 in the eastern reaches to more than 1.5 along more gently sloping western downstream reaches. Numerous small first-order drainages, many of which are deeply incised, line the banks of each stream.

Flow in these streams originates largely as runoff from rainfall and snowmelt. In mid-July 2018, the lower reaches of Deep Gulch contained sporadic pools of standing water separated by intermittent dry sections, tens of meters in length. However, the same reaches contained near bankfull flows the next day following a series of intense thunderstorms that began during the previous evening and continued for several hours. In addition to runoff, these streams receive small flows from widely scattered in-channel and near-channel springs and seeps (low magnitude discharge springs), discussed in the following section.

Hydrogeology

The Garden Gulch quadrangle contains several dozen springs, most of which discharge from the alluvium or mixed alluvial/colluvial deposits that line the streambeds. Although many springs discharge less than 0.003 m^3/s (0.1 ft^3/s), these are important water sources for livestock and wildlife in this semi-arid environment. We sampled water and natural gas from many of these springs; results are reported in Appendix 3. We observed the following types of springs (Springer and Stevens, 2008) in the Garden Gulch quadrangle:

- Rheocrene springs, flowing springs that discharge into a stream channel, are the most common type of spring encountered in the quadrangle (fig. 11). Many of these seeps are reabsorbed in-channel within a few meters of discharge during dry periods. These frequently discharge where a small first-order drainage enters the main streambed.

- Hanging garden springs are dripping or seeping (diffuse) discharges from exposed rock faces. Small hanging garden springs discharge from Almond Formation exposures (fig. 12) on large first-order tributaries to Garden Gulch and Wild Cow Creek.

- Fountain springs driven by methane pressures are distributed along the western portion of the Garden Gulch quadrangle where alluvial streambeds cross outcrops of Lewis Shale (McLaughlin, 2009). Methane-discharging springs include craters that constantly discharge spring flow (fig. 13), rising springs that discharge periodically (fig. 14), bubbling mud pots (fig. 15), and flowing wells (fig. 16). Clusters of methane-discharging springs are located near the confluence of Cow Creek and Deep Gulch, and along the lower reaches of Wild Cow Creek. Both clusters are generally on trend with the westward strike of normal faults that lie just north of Cow Creek and Deep Gulch.

Figure 11. Photograph of a rheocrene spring discharging to Deep Gulch on the eastern edge of the Garden Gulch quadrangle. The spring flows from the base of a hillside located at the mouth of an ephemeral tributary that has incised a small canyon through the Almond Formation into the Allen Ridge Formation (sample location GG-S10).

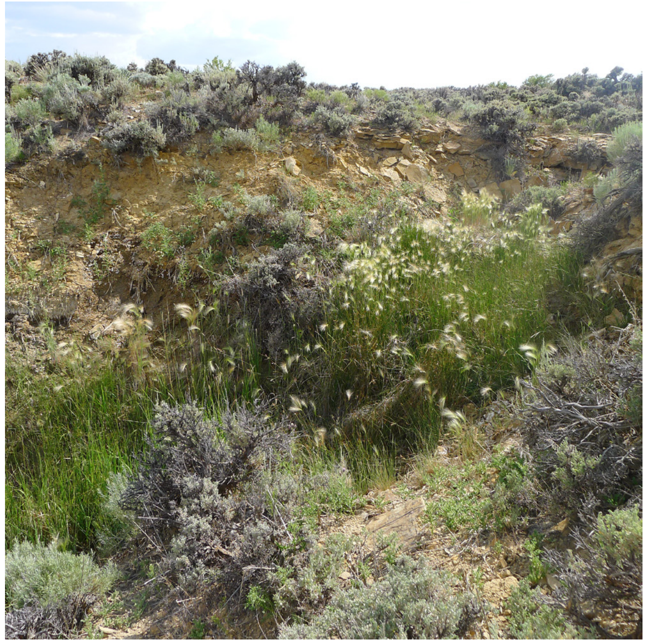

Figure 12. Photograph of a hanging-garden spring that seeps water at the Lewis Shale-Almond Formation contact on a second-order tributary to a lower reach of Wild Cow Creek (sample location GG-S08).

Figure 13. Photograph of a large circular spring, approximately 27 m (90 ft) in diameter, that continuously discharges methane and water near Cow Creek (sample location GG-S01W). Turbulence generated from methane discharge is sufficient to cause a strong circular current. Discharged spring water flows about 122 m (400 ft) to Cow Creek.

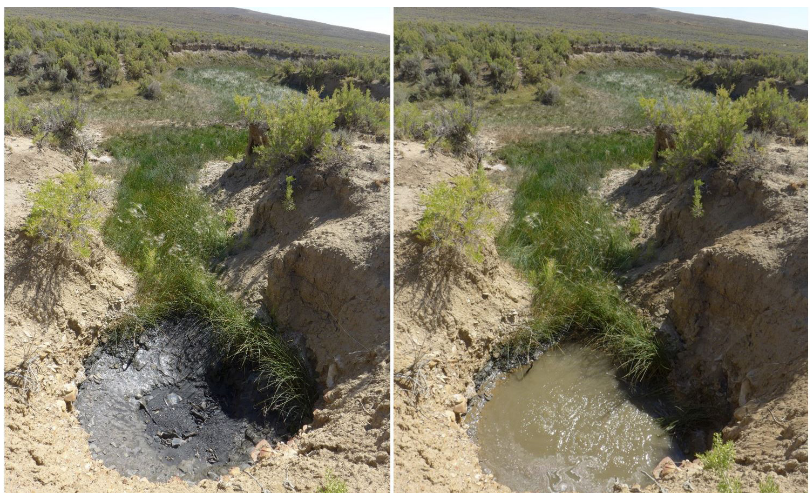

Figure 14. Photograph of a dry basin (left) of a rising spring that periodically fills with water and methane (right) from the vents seen at its center. The filled spring, about 3 m (10 ft) in diameter, bubbles vigorously for several minutes before the water level sinks below the ground surface (sample location GG-S11). Discharged water flows to the channel of Deep Gulch, about 15 m (50 ft) away.

Figure 15. Photograph of a small (1.5 m [5 ft] in diameter) bubbling mud pot that continuously discharges methane near the confluence of Cow Creek and Deep Gulch (sample location GG-S03). This spring has no outlet and may only represent a focused methane seep at the alluvial groundwater surface. Pothole-type springs like this are common in alluvial deposits throughout the Garden Gulch quadrangle, although many of them were dry in mid-July 2018.

Figure 16. Photograph of a flowing well on Deep Gulch that discharges methane continuously and water periodically (well API 49-007-05072, sample location GG-S02). When this picture was taken in mid-July 2018, this well discharged water during 6-minute intervals that alternated with 20-minute periods of quiescence. After discharging, the water level remained about 0.6 m (2 ft) below the top of the casing. Methane bubbles through the water column continuously during quiescent periods, building in intensity until water discharges from the casing again.

REFERENCES

Aslan, Andres, Boraas-Connors, Marisa, Sprinkel, Doug, Becker, T.P., Lynds, Ranie, Karlstrom, K.E., and Heizler, Matt, 2017, Cenozoic collapse of the eastern Uinta Mountains and drainage evolution of the Uinta Mountains region: Geosphere, v. 13, no. 6, p. 1–26, doi:10.1130/GES01523.1.

Bader, J.W., 2008, Structural and tectonic evolution of the Cherokee Ridge arch, south-central Wyoming—Implications for recurring strike-slip along the Cheyenne Belt suture zone: Rocky Mountain Geology, vol. 43, p. 23–40.

Barlow, J.A., 1961, Almond Formation and lower Lewis Shale, east flank of Rock Springs Uplift, Sweetwater County, Wyoming, in G. J. Wiloth, ed., Symposium of Late Cretaceous rocks of Wyoming: Wyoming Geological Association, p. 113–115.

Carroll, C.J., Spaeth, L.J., and Carnes, J.D., 2016, Preliminary geologic map of the Dixon quadrangle, Carbon County, Wyoming, and Moffat County, Colorado: Wyoming State Geological Survey Open File Report 2016-5, 33 p., 1 pl., scale 1:24,000.

Dames & Moore, 1979, Coal resource occurrence and coal development potential maps of the Doty Mountain 15-minute quadrangle, Carbon County, Wyoming: U.S. Geological Survey Open-File Report 79-1032, 28 p., 28 pls., scale 1:24,000.

Dickinson, W.R., and Gehrels, G.E., 2009, Use of U-Pb ages of detrital zircons to infer maximum depositional ages of strata—A test against a Colorado Plateau Mesozoic database: Earth and Planetary Science Letters, v. 288, p. 115–125.

Gehrels, G.E., Valencia, V.A., and Pullen, Alex, 2006, Detrital zircon geochronology by laser-ablation multicollector ICPMS at the Arizona LaserChron Center: The Paleontological Society Papers, v. 12, p. 67–76.

Gehrels, G.E., Valencia, V.A., and Ruiz, Joaquin, 2008, Enhanced precision, accuracy, efficiency, and spatial resolution of U-Pb ages by laser ablation-multicollector-inductively coupled plasma-mass spectrometry: Geochemistry, Geophysics, Geosystems, v. 9, no. 3, 13 p.

Gill, J.R., and Cobban, W.A., 1966, Regional unconformity in Late Cretaceous, Wyoming: U.S. Geological Survey Professional Paper 550-B, p. B20–B27.

Gill, J.R., Merewether, F.A., and Cobban, W.A., 1970, Stratigraphy and nomenclature of some Upper Cretaceous and Lower Tertiary rocks in south-central Wyoming: U.S. Geological Survey Professional Paper 667, 53 p.

Gomez-Veroiza, C.A., and Steel, R.J., 2010, Iles clastic wedge development and sediment partitioning within a 300-km fluvial to marine Campanian transect (3 m.y.), Western Interior seaway, southwestern Wyoming and northern Colorado: AAPG Bulletin, v. 94, p. 1,349–1,377.

Haacke, J.E., Barclay, C.S.V., and Hettinger, R.D., 2016, Preliminary geologic mapping of Cretaceous and Tertiary formations in the eastern part of the Little Snake River coal field, Carbon County, Wyoming: U.S. Geological Survey Open-File Report 2016-1170, 9 p.

Hettinger, R.D., and Honey, J.G., 2005, Geologic map and coal stratigraphy of the Blue Gap quadrangle, eastern Washakie Basin, Carbon County, Wyoming: U.S. Geological Survey Scientific Investigations Map 2878, 2 sheets, scale 1:24,000.

Hettinger, R.D., and Honey, J.G., 2006, Geologic map and coal stratigraphy of the Doty Mountain quadrangle, eastern Washakie Basin, Carbon County, Wyoming: U.S. Geological Survey Scientific Investigations Map 2925, 2 sheets, scale 1:24,000.

Hettinger, R.D., Honey, J.G., Ellis, M.S., Barclay, C.S.V., and East, J.A., 2008, Geologic map of the Upper Cretaceous and Tertiary strata and coal stratigraphy of the Paleocene Fort Union Formation, Rawlins-Little Snake River area, south-central Wyoming: U.S. Geological Survey Scientific Investigations Map 3053, 3 sheets, scale 1:100,000.

Honey, J.G., and Hettinger, R.D., 2004, Geologic map of the Peach Orchard Flat quadrangle, Carbon County, Wyoming, and descriptions of new stratigraphic units in the Upper Cretaceous Lance Formation and Paleocene Fort Union Formation, eastern Greater Green River Basin, Wyoming-Colorado: U.S. Geological Survey Scientific Investigations Map 2835, version 1.1, 9 p., 2 sheets, scale 1:24,000.

Izett, G.A., Denson, N.M., and Obradovich, J.D., 1970, K-Ar age of the lower part of the Browns Park Formation, northwestern Colorado: U.S. Geological Survey Professional Paper 700-C, p. C150–C152.

Kauffman, E.G., and Caldwell, W.G.E., 1993, The Western Interior Basin in space and time: Geological Association of Canada, Special Paper 39, 30 p.

Luo, Hongjun, 2005, Tectonostratigraphy of foreland basins—The Upper Cretaceous in southwestern Wyoming: Laramie, University of Wyoming, Ph.D. thesis, 284 p.

Luo, Hongjun, and Nummedal, Dag, 2010, Late Cretaceous stratigraphy and tectonics across southwestern Wyoming: The Mountain Geologist, v. 47, p. 91–116.

Martinsen, O.J., Ryseth, Alf, Helland-Hansen, W.H., Flesche, Harald, Torkildsen, Geir, and Idil, Sahire, 1999, Stratigraphic base level and fluvial architecture: Ericson Sandstone (Campanian), Rock Springs Uplift, SW Wyoming, USA: Sedimentology, v. 46, p. 235–259.

McLaughlin, J.F., 2009, Stable and radiogenic isotopic analysis of aquifer systems, Atlantic Rim, Carbon County, Wyoming: Implications for production of coal bed natural gas: Laramie, University of Wyoming, M.S. thesis, 76 p., 1 pl.

Merewether, E.A., 1971, Geologic map of the Wild Horse Mountain quadrangle, Carbon County, Wyoming: U.S. Geological Survey Geologic Quadrangle Map GQ-887, scale 1:24,000.

Montagne, John, 1991, Cenozoic history of the Saratoga Valley area, Wyoming and Colorado: Rocky Mountain Geology, v. 29, p. 13–70.

Pecha, Mark, 2019, Lynds Jan 2019 Element 2 Final Report—Report to Ranie Lynds, WSGS: Arizona LaserChron Center, final report.

Reynolds, M.W., 1967, Physical evidence for Late Cretaceous unconformity, south-central Wyoming: U.S. Geological Survey Professional Paper 575-D, p. D24–D28.

Roehler, H.W., 1990, Stratigraphy of the Mesaverde Group in the central and eastern Greater Green River Basin, Wyoming, Colorado, and Utah: U.S. Geological Survey Professional Paper 1508, 52 p.

Roehler, H.W., 1992, Introduction to Greater Green River Basin geology, physiography, and history of investigations: U.S. Geological Survey Professional Paper 1506-A, 14 p.

Scott, J.E., Sutherland, W.M., Johnson, Joe, and McLaughlin, J.F., 2011, Geologic map of the Baggs 30’ x 60’ quadrangle, Carbon and Sweetwater counties, Wyoming, and Moffat and Routt counties, Colorado: Wyoming State Geological Survey Map Series 95, scale 1:100,000.

Slattery, J.S., Cobban, W.A., McKinney, K.C., Harries, P.J., and Sandness, A.L., 2015, Early Cretaceous to Paleocene paleogeography of the Western Interior Seaway—The interaction of eustasy and tectonism: Wyoming Geological Association, 68th annual field conference, Guidebook, p. 22–60.

Springer, A.E., and Stevens, L.E., 2008, Spheres of discharge of springs: Hydrogeology Journal v. 17, no. 1, p 83–93.

Stacey, J.S., and Kramers, J.D., 1975, Approximation of terrestrial lead isotope evolution by a two-stage model: Earth and Planetary Science Letters, v. 26, p. 207–221.

Steidtmann, J.R., 1993, The Cretaceous foreland basin and its sedimentary record, in Snoke, A.W., Steidtmann, J.R., and Roberts, S.M., eds., Geology of Wyoming: Geological Survey of Wyoming [Wyoming State Geological Survey] Memoir 5, p. 250–271.

Sutherland, W.M., Stafford, J.E., Carroll, C.J., Gregory, R.W., and Kehoe, K.S., 2018, Mines and Minerals Map of Wyoming: Wyoming State Geological Survey, accessed March 2019, at http://wsgs.maps.arcgis.com/apps/webappviewer/index.html?id=af948a51f4954a81adeae8935440cd28.

Wilson, A.B., 2015, Uranium in the Wyoming Landscape Conservation Initiative Study Area, southwestern Wyoming: U.S. Geological Survey Open-File Report 2014–1123, 33 p., 1 pl., http://dx.doi.org/10.3133/ofr20141123.

WOGCC, 2019, Wyoming Oil and Gas Conservation Commission, accessed March 2019, at http://wogcc.state.wy.us/.

Appendix 1

Appendix 1: Detrital Zircon Geochronology

U-Pb Methodology

Detrital zircon geochronology analyses were carried out at the Arizona LaserChron Center at the University of Arizona, and the following text is modified from Pecha (2019). Zircon grains were extracted from bulk sample, including density separation using a Wilfley table and heavy liquids (methylene iodide). The resulting heavy mineral fraction then underwent separation using a Frantz LB-1 magnetic barrier separator to isolate the zircons. A representative split of the entire zircon yield of each sample was incorporated into a 1-inch epoxy mount along with multiple fragments of each of the three zircon standards (FC1, SL-mix, and R33). The mounts were sanded down approximately 20 microns, polished progressively using 9-, 5-, 3-, and 1-micron polishing pads, and backscatter electron (BSE) imaged using a Hitachi S-3400N scanning electron microscope (SEM) equipped with a Gatan Chroma CL2 detector. Prior to isotopic analysis, the mounts were cleaned in an ultrasound bath of 1 percent HNO_3 and 1 percent HCl in order to remove any residual common Pb from the surface of the mount.

U-Pb geochronology of individual zircon crystals was conducted by laser ablation multicollector inductively coupled mass spectrometry (LA-ICPMS) at the Arizona LaserChron Center (Gehrels and others, 2006, 2008). The isotopic analyses involved ablation of zircon using a Photon Machines Analyte G2 excimer laser coupled to a Thermo Element 2 single-collector-ICPMS. Drill rate is approximately one micron per second, resulting in a final ablation pit depth of about 12 microns.

The errors in determining the $^{206}Pb/^{238}U$ and $^{206}Pb/^{204}Pb$ result in a final measurement error of approximately 1–2 percent (at 2σ level) in the $^{206}Pb/^{238}U$ age for each analysis. The errors in determining $^{206}Pb/^{207}Pb$ and $^{206}Pb/^{204}Pb$ also result in approximately 1–2 percent (at 2σ level) uncertainty in age for grains that are older than 900 Ma, however, they are substantially larger for younger grains due to the low intensity of the ^{207}Pb signal.

The common Pb correction is accomplished by using the Hg-corrected ^{204}Pb and assuming an initial Pb composition from Stacey and Kramers (1975). Uncertainties of 1.5 for $^{206}Pb/^{204}Pb$ and 0.3 for $^{207}Pb/^{204}Pb$ are applied to these compositional values based on the variation in Pb isotopic composition in modern crystalline rocks. Interference of ^{204}Hg with ^{204}Pb is accounted for measurement of ^{202}Hg during laser ablation and subtraction of ^{204}Hg, according to the natural $^{202}Hg/^{204}Hg$ of 4.35.

U-Pb Results

Tables A1–1 and A1–2 summarize detrital zircon data from samples of the Browns Park Formation (basal sandstone; GG-Tbp-01g) and Allen Ridge Formation (lower member; GG-Karl_01g). The locations of samples GG-Tbp-01g and GG-Karl_01g are shown on the map, and all sample locations are summarized in table A1–1.

For each sample, maximum depositional age was calculated by multiple methods following Dickinson and Gehrels (2009), with results summarized in table A1–1. Youngest single grain (YSG) is the absolute youngest age measured in a sample. The probability density peak (PDP) age was calculated from the crest of the youngest discrete age peak on a probability density plot. Final age (FA), or age incorporating both internal analytical error accounted for with the weighted mean age and external systematic error, was calculated using the DZ Age Pick Program (version of September 1, 2009) of the Arizona LaserChron Center (www.geo.arizona.edu/alc). The weighted mean age at 2σ was determined from the youngest cluster of three or more grain ages ($i \geq 3$) overlapping in age by weighting each measurement by the square of its uncertainty. This method assumes the grains are cogenetic and is valid if the mean square weighted deviation (MSWD) of the set of grains is near one.

Compiled single zircon age results for the two samples summarized in table A1–1 are reported in table A1–2. Uncertainties shown in these results are at the 1σ level and include only measurement errors. Complete digital analytical data are available from the Wyoming State Geological Survey (www.wsgs.wyo.gov).

Table A1–1. Samples processed for detrital zircon U-Pb age dates. Latitude and longitude are displayed in GCS NAD27; *n* represents the number of zircons analyzed for each sample. Maximum depositional age (Ma) calculated by multiple methods following Dickinson and Gehrels (2009), including youngest single grain (YSG ± 1σ), probability density peak (PDP), and final age (FA [*i*], at 95 percent confidence, where *i* indicates the actual number of grains included in the cluster). MSWD is the mean square weighted deviation.

Sample Name	Formation	Latitude	Longitude	*n*	YSG	PDP	FA (*i*)	MSWD
GG-Tbp-01g	Tbp	41.31970	-107.50688	303	25.8 ± 0.3	28.9	28.69 ± 0.21 (26)	1.7
GG-Karl-01g	Karl	41.28826	-107.50767	298	75.9 ± 0.7	76.4	76.92 ± 1.03 (5)	1.2

Table A1–2. Compiled detrital zircon best ages (Ma; 1σ) for the two samples summarized in table A1–1. Complete digital analytical data table available from the Wyoming State Geological Survey (www.wsgs.wyo.gov).

GG-Tbp-01g	GG-Karl-01g
25.8 ± 0.3	75.9 ± 0.7
27.7 ± 0.4	76.3 ± 1.0
27.7 ± 0.5	77.2 ± 1.0
28.1 ± 0.3	77.7 ± 1.2
28.1 ± 0.3	78.0 ± 0.8
28.1 ± 0.5	81.1 ± 1.0
28.2 ± 0.4	83.7 ± 1.1
28.6 ± 0.4	86.4 ± 1.0
28.7 ± 0.5	87.5 ± 1.1
28.7 ± 0.5	88.1 ± 1.5
28.7 ± 0.4	88.2 ± 1.0
28.7 ± 0.3	88.3 ± 0.9
28.7 ± 0.5	88.4 ± 1.1
28.7 ± 0.4	88.6 ± 1.0
28.7 ± 0.4	89.3 ± 1.2
28.8 ± 0.5	89.7 ± 1.0
28.8 ± 0.4	90.7 ± 1.2
29 ± 0.5	90.8 ± 1.3
29 ± 0.4	91.2 ± 1.3
29.1 ± 0.4	91.4 ± 1.2
29.1 ± 0.4	91.5 ± 1.2
29.1 ± 0.4	91.6 ± 1.1
29.2 ± 0.5	92.1 ± 0.9
29.3 ± 0.4	92.3 ± 1.3
29.5 ± 0.5	93.4 ± 0.8
29.5 ± 0.4	93.4 ± 1.1
29.5 ± 0.4	93.8 ± 1.4
29.7 ± 0.3	94.1 ± 1.2
29.8 ± 0.3	94.2 ± 1.0

Table A1–2 continued.

GG-Tbp-01g	GG-Karl-01g
29.9 ± 0.4	94.3 ± 1.4
30.1 ± 0.4	94.3 ± 1.2
30.1 ± 0.5	94.3 ± 1.0
30.2 ± 0.5	94.4 ± 1.2
30.3 ± 0.4	94.6 ± 0.9
30.5 ± 0.4	94.7 ± 1.1
30.5 ± 0.4	94.9 ± 1.4
30.5 ± 0.3	94.9 ± 1.3
30.7 ± 0.5	95.9 ± 1.1
30.8 ± 0.4	96.0 ± 1.1
31.2 ± 0.4	96.1 ± 1.3
31.3 ± 0.4	96.3 ± 1.1
31.4 ± 0.4	96.4 ± 1.1
31.8 ± 0.5	96.7 ± 0.8
32.0 ± 0.4	97.0 ± 1.5
32.1 ± 0.4	97.4 ± 1.0
32.3 ± 0.5	97.5 ± 1.0
32.7 ± 0.4	98.9 ± 1.0
32.8 ± 0.5	99.0 ± 1.5
32.8 ± 0.4	100.2 ± 1.3
33.0 ± 0.3	100.2 ± 1.5
33.0 ± 0.4	100.8 ± 1.2
33.2 ± 0.5	114.4 ± 1.3
33.2 ± 0.6	142.3 ± 1.5
33.5 ± 0.4	159.5 ± 2.0
33.9 ± 0.5	270.6 ± 2.6
33.9 ± 0.5	404.7 ± 4.5
34.0 ± 0.5	411.7 ± 4.4
34.1 ± 0.4	413.1 ± 4.4

Table A1–2 continued.

GG-Tbp-01g	GG-Karl-01g
34.1 ± 0.4	430.7 ± 3.9
34.1 ± 0.4	432.6 ± 5.7
34.2 ± 0.4	441.6 ± 5.4
34.2 ± 0.4	441.8 ± 5.1
34.4 ± 0.4	449.2 ± 4.7
34.5 ± 0.4	464.6 ± 4.6
34.5 ± 0.5	469.3 ± 5.5
34.5 ± 0.5	478.9 ± 5.4
34.6 ± 0.4	502.8 ± 5.7
34.7 ± 0.5	505.3 ± 6.2
34.7 ± 0.4	512.6 ± 7.4
34.7 ± 0.4	563.7 ± 6.2
34.8 ± 0.6	614.6 ± 7.6
34.9 ± 0.6	665.6 ± 6.0
34.9 ± 0.5	751.4 ± 6.8
34.9 ± 0.4	956.8 ± 18.2
34.9 ± 0.5	961.2 ± 33.3
34.9 ± 0.6	984.5 ± 15.0
35.2 ± 0.5	988.0 ± 13.9
35.2 ± 0.5	992.2 ± 19.8
35.5 ± 0.4	1,022.0 ± 13
35.7 ± 0.6	1,047.1 ± 17.5
35.7 ± 0.5	1,053.5 ± 15.0
35.7 ± 0.5	1,053.7 ± 15.2
35.7 ± 0.5	1,071.3 ± 14.6
35.9 ± 0.6	1,073.6 ± 15.2
36.1 ± 0.6	1,091.5 ± 16.3
36.1 ± 0.4	1,097.1 ± 17.4
36.2 ± 0.5	1,107.1 ± 16.2

Table A1–2 continued.

GG-Tbp-01g	GG-Karl-01g
36.3 ± 0.5	1,113 ± 15.2
36.5 ± 0.6	1,117.5 ± 15.3
36.5 ± 0.7	1,121.6 ± 28.0
36.7 ± 0.6	1,123.4 ± 19.9
36.8 ± 0.5	1,125.9 ± 19.3
37.1 ± 0.5	1,176.8 ± 13.3
37.7 ± 0.6	1,181.7 ± 16.1
38.3 ± 0.6	1,216.7 ± 16.8
40.1 ± 0.7	1,252.1 ± 15.3
40.8 ± 0.7	1,253.3 ± 15.2
41.8 ± 0.5	1,253.7 ± 16.0
41.8 ± 0.7	1,277.9 ± 33.7
42.0 ± 0.4	1,306.7 ± 18.6
42.1 ± 0.7	1,336.2 ± 17.5
44.8 ± 0.7	1,341.4 ± 16.5
45.2 ± 0.7	1,353.4 ± 15.3
46.3 ± 0.5	1,366 ± 11.8
47.0 ± 0.5	1,370.7 ± 12.9
48.0 ± 0.9	1,373.3 ± 16.6
50.2 ± 0.6	1,374.7 ± 16.0
57.0 ± 0.5	1,393.7 ± 13.7
59.3 ± 0.9	1,416.6 ± 12.0
59.4 ± 0.6	1,424.2 ± 15.3
59.5 ± 1.1	1,424.8 ± 17.4
60.2 ± 0.6	1,433.7 ± 14.5
65.4 ± 1.0	1,440.3 ± 16.0
72.7 ± 1.1	1,445.8 ± 10.9
72.9 ± 1.0	1,449.8 ± 21.7
74.4 ± 1.2	1,453.7 ± 15.0
74.9 ± 0.7	1,475.8 ± 21.8
85.0 ± 0.8	1,484.6 ± 13.7
90.2 ± 1.0	1,507.6 ± 10.8
96.0 ± 1.8	1,540 ± 14.1
97.5 ± 1.1	1,547.9 ± 12.9
102.3 ± 1.5	1,553.9 ± 13.4
127.3 ± 1.6	1,575.0 ± 15.5
159.3 ± 2.1	1,623.1 ± 13.8
163.4 ± 2.2	1,624.0 ± 10.8
164.2 ± 2.2	1,633.4 ± 14.6
169.5 ± 1.8	1,634.9 ± 15.3
173.9 ± 2.2	1,638.3 ± 10.5
175.5 ± 6.2	1,639.9 ± 13.3

Table A1–2 continued.

GG-Tbp-01g	GG-Karl-01g
177 ± 2.6	1,649.3 ± 14.2
192.4 ± 2.2	1,653.3 ± 13.0
221.7 ± 2.1	1,655.0 ± 10.6
224.1 ± 2.0	1,656.1 ± 15.1
260.5 ± 3.1	1,657.9 ± 12.5
270.3 ± 3.0	1,659.5 ± 15.9
368.5 ± 4.9	1,659.5 ± 15.2
369.4 ± 4.2	1,662.5 ± 14.3
374.6 ± 4.7	1,663.6 ± 12.1
393.7 ± 3.9	1,670.1 ± 15.0
409.8 ± 5.0	1,673.4 ± 13.0
415.0 ± 3.7	1,677.1 ± 15.3
420.2 ± 5.3	1,679.5 ± 15.3
423.5 ± 4.2	1,680.2 ± 11.3
439.6 ± 5.5	1,681.2 ± 14.7
487.1 ± 5.8	1,681.7 ± 12.1
497.7 ± 5.9	1,682.2 ± 14.5
632.5 ± 6.2	1,683.2 ± 10.7
632.6 ± 9.4	1,684.1 ± 13.5
639.1 ± 7.6	1,684.6 ± 16.8
935.5 ± 17.5	1,684.6 ± 12.6
944.4 ± 22.7	1,685.0 ± 13.7
971.5 ± 19.1	1,687.8 ± 19.7
986.7 ± 21.7	1,689.0 ± 15.5
991.9 ± 16.6	1,689.5 ± 13.0
1,003.5 ± 15.2	1,691.3 ± 13.3
1,004.2 ± 23.9	1,691.9 ± 12.0
1,008.3 ± 18.9	1,692.6 ± 13.1
1013.5 ± 20.6	1,693.1 ± 12.5
1,028.4 ± 18.2	1,695.2 ± 11.8
1,048.5 ± 17.4	1,695.7 ± 14.8
1,055.3 ± 29.7	1,695.8 ± 15.1
1,059 ± 14.4	1,696.0 ± 11.2
1,066.9 ± 23.0	1,696.7 ± 15.8
1,067.5 ± 18.4	1,699.4 ± 13.9
1,068.0 ± 17.0	1,699.5 ± 12.0
1,079.6 ± 32.9	1,700.0 ± 15.5
1,089.5 ± 17.0	1,700.1 ± 14.0
1,110.7 ± 16.7	1,700.7 ± 19.0
1,113.1 ± 20.4	1,701.2 ± 16.1
1,116.5 ± 15.6	1,702.6 ± 14.7
1,117.2 ± 26	1,703.6 ± 11.7

Table A1–2 continued.

GG-Tbp-01g	GG-Karl-01g
1,161.4 ± 19.0	1,704.2 ± 11.5
1,167.2 ± 18.2	1,704.8 ± 17.4
1,189.2 ± 19.0	1,706.6 ± 15.1
1,189.4 ± 35.5	1,706.9 ± 12.7
1,198.8 ± 16.3	1,707.2 ± 14.0
1,214.0 ± 19.7	1,707.7 ± 16.1
1,279.6 ± 15.7	1,707.8 ± 16.7
1,393.6 ± 11.0	1,708.8 ± 13.1
1,409.7 ± 20.5	1,708.9 ± 12.4
1,410.8 ± 14.0	1,709.3 ± 13.5
1,411.9 ± 15.3	1,709.6 ± 14.2
1,412.8 ± 15.7	1,711 ± 10.5
1,414.3 ± 15.2	1,711.6 ± 14.3
1,418.1 ± 21.3	1,711.9 ± 11.0
1,418.9 ± 19.3	1,713.2 ± 12.7
1,419.1 ± 16.8	1,714.0 ± 13.8
1,425.1 ± 15.2	1,717.5 ± 11.5
1,425.7 ± 15.1	1,718.1 ± 12.4
1,425.8 ± 15.2	1,718.3 ± 13.4
1,426.0 ± 11.9	1,718.7 ± 13.1
1,426.1 ± 14.5	1,719.6 ± 11.0
1,426.5 ± 19.2	1,719.7 ± 16.5
1,426.8 ± 19.0	1,720.3 ± 15.1
1,427.5 ± 19.0	1720.9 ± 14.2
1,428.1 ± 17.7	1,721.2 ± 14.0
1,429.4 ± 17.3	1,722.8 ± 13.5
1,431.1 ± 17.4	1,722.8 ± 12.7
1,433.1 ± 18.0	1,724.5 ± 14.0
1,433.4 ± 16.3	1,725.0 ± 13.9
1,435.2 ± 21.3	1,725.8 ± 12.7
1,439.2 ± 13.0	1,725.8 ± 13.7
1,443.4 ± 19.1	1,728.6 ± 15.1
1,443.5 ± 17.9	1,728.9 ± 14.6
1,444.8 ± 14.9	1,729.2 ± 13.2
1,446.6 ± 18.0	1,729.4 ± 10.8
1,449.6 ± 15.7	1,730.4 ± 12.4
1,449.7 ± 16.3	1,731.0 ± 14.8
1,451.1 ± 15.7	1,731.1 ± 12.8
1,451.7 ± 23.1	1,732.6 ± 12.0
1,451.9 ± 14.7	1,732.8 ± 11.8
1,456.0 ± 16.9	1,734.1 ± 21.7
1,458.0 ± 14.5	1,736.4 ± 13.5

Table A1–2 continued.

GG-Tbp-01g	GG-Karl-01g
1,461.7 ± 14.1	1,737.2 ± 14.9
1,472.3 ± 16.4	1,738.9 ± 10.6
1,473.3 ± 17.5	1,740.2 ± 14.8
1,475.7 ± 16.0	1,741.5 ± 13.8
1,539.9 ± 25.0	1,746.5 ± 11.6
1,603.9 ± 14.6	1,747.6 ± 17.4
1,613.8 ± 14.1	1,747.9 ± 13.0
1,640.5 ± 15.3	1,748.8 ± 11.9
1,643.3 ± 14.3	1,754.5 ± 13.2
1,647.0 ± 13.4	1,755.3 ± 16.5
1,650.6 ± 14.9	1,756.0 ± 15.7
1,656.0 ± 22.7	1,756.2 ± 16.9
1,657.2 ± 16.9	1,756.3 ± 13.4
1,657.3 ± 14.1	1,757.4 ± 12.5
1,658.1 ± 16.1	1,757.7 ± 11.4
1,661.1 ± 13.0	1,758.8 ± 13.6
1,663.4 ± 14.5	1,763.1 ± 15.2
1,666.4 ± 16.6	1,764.7 ± 12.7
1,666.7 ± 13.1	1,765.0 ± 10.3
1,668.4 ± 16.5	1,765.5 ± 15.6
1,670.9 ± 16.3	1,766.8 ± 13.3
1,671.8 ± 12.4	1,767.5 ± 13.3
1,676.2 ± 16.7	1,767.8 ± 13.0
1,680.3 ± 17.3	1,768.5 ± 33.2
1,681.3 ± 13.1	1,774.9 ± 11.2
1,681.7 ± 11.6	1,778.5 ± 13.6
1,684.5 ± 15.1	1,779.3 ± 12.2
1,685.9 ± 13.1	1,783.4 ± 9.6
1,687.1 ± 12.1	1,786.1 ± 15.8
1,690.1 ± 16.7	1,787.0 ± 25.6

Table A1–2 continued.

GG-Tbp-01g	GG-Karl-01g
1,692.5 ± 14.5	1,787.9 ± 27.1
1,693.0 ± 15.1	1,788.9 ± 15.3
1,693.4 ± 15.0	1,795.9 ± 12.9
1,695.0 ± 19.8	1,802.0 ± 12.5
1,697.0 ± 16.6	1,805.8 ± 16.5
1,697.8 ± 14.2	1,817.9 ± 10.4
1,698.4 ± 17.8	1,823.2 ± 15.3
1,699.5 ± 14.5	1,823.3 ± 15.5
1,699.6 ± 13.3	1,825.7 ± 14.8
1,700.5 ± 13.3	1,828.3 ± 19.5
1,701.0 ± 11.3	1,834.8 ± 11.5
1,701.9 ± 15.4	1,839.7 ± 15.8
1,704.2 ± 15.9	1,841.5 ± 12.3
1,705.1 ± 14.6	1,843.9 ± 12.5
1,705.7 ± 14.3	1,847.9 ± 12.7
1,706.2 ± 13.0	1,848.0 ± 13.7
1,707.0 ± 19.0	1,848.7 ± 13.0
1,708.0 ± 15.3	1,858.3 ± 10.7
1,710.5 ± 14.9	1,867.7 ± 14.9
1,713.1 ± 13.1	1,878.4 ± 13.4
1,718.5 ± 14.1	1,901.1 ± 12.2
1,719.2 ± 14.3	1,905.6 ± 11.5
1,720.3 ± 13.0	1,931.6 ± 13.0
1,722.2 ± 17.0	1,942.0 ± 12.3
1,727.0 ± 12.9	1,943.1 ± 9.6
1,727.3 ± 14.0	1,958.1 ± 13.8
1,736.0 ± 12.9	1,961.4 ± 15.9
1,740.0 ± 16.6	1,962.0 ± 10.9
1,746.9 ± 14.3	2,045.7 ± 13.0
1,749.2 ± 13.1	2,062.7 ± 13.7

Table A1–2 continued.

GG-Tbp-01g	GG-Karl-01g
1,752.4 ± 15.1	2,112.8 ± 24.3
1,754.6 ± 15.6	2,182.3 ± 13.9
1,769.2 ± 13.9	2,365.3 ± 10.5
1,771.1 ± 15.0	2,395.3 ± 12.4
1,780.0 ± 12.2	2,416.9 ± 12.7
1,789.0 ± 12.2	2,471.5 ± 11.8
1,804.2 ± 13.8	2,479.2 ± 13.0
1,809.4 ± 14.9	2,525.5 ± 11.3
1,849.8 ± 15.2	2,568.7 ± 12.1
1,853.2 ± 11.5	2,571.7 ± 13.4
1,880.2 ± 17.1	2,572.4 ± 17.1
2,027.6 ± 15.3	2,580.7 ± 13.5
2,088.3 ± 11.1	2,639.6 ± 13.8
2,088.7 ± 14.2	2,644.9 ± 13.2
2,226.0 ± 14.2	2,651.5 ± 10.5
2,233.3 ± 15.0	2,658.8 ± 10.1
2,393.0 ± 327.1	2,663.4 ± 12.5
2,631.1 ± 12.5	2,672.7 ± 12.4
2,635.5 ± 12.7	2,673.1 ± 10.6
2,658.6 ± 15.6	2,685.1 ± 13.4
2,686.2 ± 10.4	2,687.5 ± 10.4
2,702.6 ± 12.0	2,702.1 ± 12.2
2,705.9 ± 14.3	2,722.8 ± 17.5
2,708.7 ± 13.6	2,740.7 ± 12.4
2,710.4 ± 13.0	3,088.8 ± 13.2
2,714.6 ± 12.0	
2,718.9 ± 14.5	
2,723.8 ± 13.2	
2,724.5 ± 11.0	
3,664.3 ± 12.1	

Appendix 2

Appendix 2: Coal Quality

Wyoming Analytical Laboratories, Inc., analyzed four coal samples collected from the Garden Gulch quadrangle for heating value, proximate, and ultimate analyses. Vitrinite reflectance for two of these samples was measured at the University of Kentucky.

Samples were collected from coal bed exposures using a hand auger in order to obtain less weathered material. Reasonable attempts were made to collect material from the entire thickness of the coal bed for a representative sample. Three of the coal samples were collected from Almond Formation coal beds, and the fourth was collected from a coal bed in the Allen Ridge Formation (table A2–1).

Table A2–1. Outcrop coal sample results for heating value, proximate, and ultimate analyses, as well as vitrinite reflectance. Results are displayed on an as-received (AR), moisture-free (Dry), and moisture- and ash-free basis (MAF). Latitude and longitude reported in GCS NAD27.

				Moisture Content	Ash Content	
Sample Name	Sample Description	Latitude	Longitude	Total AR (%)	AR (%)	Dry (%)
GG-Kal-01c	Robertson coal	41.31554	-107.56977	8.79	24.27	26.61
GG-Kal-02c	Garden Gulch coal	41.33553	-107.57335	28.76	4.8	6.74
GG-Kal-03c	Almond Formation, unnamed coal	41.31530	-107.58087	22.98	13.81	17.93
GG-Karu-01c	upper Allen Ridge Formation	41.28074	-107.51781	30.91	7.98	11.55

	Volatile Matter			Fixed Carbon			Sulfur Content		
Sample Name	AR (%)	Dry (%)	MAF (%)	AR (%)	Dry (%)	MAF (%)	AR (%)	Dry (%)	MAF (%)
GG-Kal-01c	33.04	36.22	49.36	33.90	37.17	50.64	0.79	0.86	1.18
GG-Kal-02c	31.84	44.74	49.97	34.54	48.53	52.03	0.24	0.33	0.36
GG-Kal-03c	32.66	42.4	51.67	30.55	39.67	48.33	0.82	1.06	1.29
GG-Karu-01c	39.97	43.38	49.04	31.14	45.07	50.96	0.38	0.55	0.62

	Heating Values (BTU)			Carbon			Hydrogen		
Sample Name	AR (%)	Dry (%)	MAF (%)	AR (%)	Dry (%)	MAF (%)	AR (%)	Dry (%)	MAF (%)
GG-Kal-01c	7,090	7,773	10,592	44.85	49.17	67.00	2.70	2.96	4.03
GG-Kal-02c	6,828	9,585	10,277	44.85	62.96	67.5	2.24	3.15	3.37
GG-Kal-03c	6,019	7,815	9,522	40.96	53.18	64.8	2.2	2.85	3.48
GG-Karu-01c	6,359	9,204	10,406	40.93	59.24	66.98	2.20	3.19	3.60

	Nitrogen			Oxygen			Vitrinite Reflectance	
Sample Name	AR (%)	Dry (%)	MAF (%)	AR (%)	Dry (%)	MAF (%)	Rmax	Rrandom
GG-Kal-01c	0.56	0.61	0.84	18.05	19.78	26.96		
GG-Kal-02c	0.98	1.38	1.48	18.13	25.45	27.29		
GG-Kal-03c	0.87	1.13	1.38	18.37	23.85	29.05	0.50	0.44
GG-Karu-01c	0.41	0.59	0.66	17.19	24.89	28.14	0.51	0.47

Appendix 3

Appendix 3: Formation Water and Gas Analyses

Water samples were acquired at 12 springs or wells that displayed either active bubbling or visible water flow. Two samples were taken from each flowing spring or well in bottles provided by the Wyoming Department of Agriculture. One water sample for major ion analysis was collected in a rinsed 800 mL plastic bottle; a second water sample for metals analysis was collected in a 200 mL plastic bottle containing nitric acid. Samples were not collected from stagnant water seeps, which are typically contaminated by livestock and wildlife use, thereby rendering any such samples unrepresentative of formation-water geochemistry. Water samples were analyzed by the Wyoming Department of Agriculture. Results are reported in table A3–1.

Table A3–1. Physical, major ion, and metals data for samples collected from selected water features in the Garden Gulch quadrangle. Laboratory analyses by Wyoming Department of Agriculture Analytical Services Lab (http://wyagric.state.wy.us/divisions/asl). More information is available on the USGS Water-Quality Information pages (https://water.usgs.gov/owq/). Latitude and longitude reported in GCS NAD27. Asterisk (*) indicates sample was delivered to the laboratory after 48-hour specified holding time expired; no valid analysis was possible for this constituent.

Sample Name	Feature Description	Date Sampled	Latitude	Longitude
GG-S01W	Large bubbling spring	07/09/18	41.33332	-107.61741
GG-S02W	Plugged and abandoned oil well, vents water and gas, API 49-007-05072	07/09/18	41.32378	-107.62049
GG-S03W	Small bubbling spring	07/09/18	41.32551	-107.62297
GG-S04W	Mud seep	07/09/18	41.35318	-107.55063
GG-S05W	Rock seep #1	07/09/18	41.33878	-107.54991
GG-S06W	Sulfur spring	07/10/18	41.25340	-107.57235
GG-S07W	Circular spring	07/10/18	41.29119	-107.60252
GG-S08W	Rock seep #2	07/10/18	41.28455	-107.60801
GG-S09W	Large bubbling spring	07/24/18	41.27436	-107.62011
GG-S10W	Cut bank trickling spring	07/25/18	41.33777	-107.51608
GG-S11W	Rising spring	09/10/18	41.32570	-107.61852
GG-S12W	Plugged and abandoned oil well, flowing water, API 49-007-05069	09/11/18	41.29890	-107.60795

Sample Name	Nitrate, mg/L	Nitrite, water, filtered, mg/L	Chloride, water, filtered, mg/L	Fluoride, water, filtered, mg/L	Sulfate, water, filtered, mg/L	Nitrate + Nitrite, water, filtered, mg/L	SC, lab, uS/cm @25 degC	Total Dissolved Solids by summation
GG-S01W	<0.20*	<0.20*	150	7.4	13	<0.20*	2,800	1,600
GG-S02W	<0.20*	<0.20*	160	6.3	<2.0	<0.20*	2,700	1,500
GG-S03W	<0.20*	<0.20*	410	8.5	71	<0.20*	5,300	2,500
GG-S04W	<0.20*	<0.20*	11	<0.50	230	<0.20*	1,300	1,100
GG-S05W	<0.20*	<0.20*	20	0.6	140	<0.20*	1,100	620
GG-S06W	<0.20*	<0.20*	14	7.6	<2.0	<0.20*	1,600	840
GG-S07W	<0.20*	<0.20*	100	9.2	11	<0.20*	3,900	1,400
GG-S08W	<0.20*	<0.20*	32	7.6	140	<0.20*	2,100	1,300
GG-S09W	0.35	<0.20*	160	10	12	0.35	3,700	1,500
GG-S10W	0.32	<0.20*	4.8	<0.5	240	0.32	1,200	690
GG-S11W	<0.20*	<0.20*	73	5.9	370	<0.20*	1,080	1,700
GG-S12W	<0.20*	<0.20*	6.3	5.3	55	<0.20*	1,600	920

Table A3–1 continued.

Sample Name	Alkalinity, water, filtered, mg/L	Bicarbonate, water, filtered, mg/L	Calcium, water, filtered, ppm	Calcium Hardness, water, filtered, mg/L	Carbonate, water, filtered, mg/L	Copper, water, filtered, ppm	Iron, water, filtered, ppm	Lead, water, filtered, ppm
GG-S01W	1,400	1,300.0	44.0	110.0	90.0	0.078	23.3	0.023
GG-S02W	1,300	1,200.0	6.88	17.0	96.0	0.043	0.098	<0.005
GG-S03W	<20	<20.0	304.0	760.0	190.0	0.049	81.5	0.061
GG-S04W	530	530.0	386.0	960.0	<2.0	<0.010	24.1	0.017
GG-S05W	460	460.0	111.0	280.0	<2.0	<0.010	0.68	<0.005
GG-S06W	870	840.0	3.67	9.2	<2.0	<0.010	0.3	<0.005
GG-S07W	<20	<20.0	16.3	41.0	250	0.029	6.92	0.011
GG-S08W	1,040	1,000.0	30.4	76.0	41.0	<0.010	0.2	<0.005
GG-S09W	<20	<20.0	44.3	110.0	210.0	0.064	22.3	0.047
GG-S10W	360	360.0	23.8	59.0	<2.0	<0.010	0.74	<0.005
GG-S11W	1,140	1,140.0	25.0	62.0	<2.0	<0.010	0.15	<0.005
GG-S12W	820	750.0	1.14	2.8	68.0	<0.010	0.085	<0.005

Sample Name	Magnesium, water, filtered, ppm	Manganese, water, filtered, ppm	pH, water, lab	Potassium, water, filtered, ppm	Sodium, water, filtered, mg/L	Total Hardness, water, filtered, mg/L	Zinc, water, filtered, ppm
GG-S01W	18.5	0.669	8.6	8.92	718.0	190.0	0.117
GG-S02W	2.01	<0.005	8.6	5.77	675.0	26.0	<0.005
GG-S03W	104.0	4.46	8.7	15.9	1,440.0	1,200.0	0.379
GG-S04W	139.0	3.54	7.7	9.98	32.5	1,500.0	0.263
GG-S05W	86.4	0.116	8.2	5.67	32.9	630.0	0.017
GG-S06W	1.97	0.006	8.4	2.73	402.0	17.0	0.006
GG-S07W	11.5	0.217	8.9	7.78	993.0	88.0	0.049
GG-S08W	43.7	0.092	8.4	1.17	471.0	260.0	<0.005
GG-S09W	11.6	0.603	8.8	8.16	994.0	160.0	0.115
GG-S10W	15.5	0.026	8.0	2.31	225.0	120.0	0.009
GG-S11W	80.4	0.017	8.1	7.59	541.0	390.0	<0.005
GG-S12W	0.35	0.007	8.7	1.66	409.0	4.3	<0.005

Gas samples were taken from four bubbling springs and one bubbling well. Samples were collected in Isojars obtained from Isotech Laboratories in compliance with its sampling procedures. The jars are approximately 600 mL in volume and contain benzalkonium chloride (a bactericide). During sample collection, the Isojars were filled with water by submersion in the spring or well, then turned upside down and filled by water displacement by the gas sample to two-thirds of capacity. The gas samples were shipped in the inverted Isojars to Isotech Laboratories for analysis. Results are reported in table A3–2.

Table A3–2. Gas composition and isotopic data for gas samples collected from selected water features in the Garden Gulch quadrangle. Laboratory analyses by Isotech Laboratories (http://www.isotechlabs.com/). Latitude and longitude reported in GCS NAD27.

Sample Name	Feature Description	Date Sampled	Latitude	Longitude
GG-S01G	Large bubbling spring	09/10/18	41.33332	-107.61741
GG-S02G	Plugged and abandoned oil well, vents water and gas, API 49-007-05072	09/10/18	41.32378	-107.62049
GG-S03G	Small bubbling spring	09/10/18	41.32551	-107.62297
GG-S06G	Sulfur spring	09/11/18	41.25340	-107.57235
GG-S09G	Large bubbling spring	09/11/18	41.27436	-107.62011

Sample Name	He (%)	H_2 (%)	Ar (%)	O_2 (%)	CO_2 (%)	N_2 (%)	CO (%)	C_1 (%)	C_2 (%)	C_2H_4 (%)	C_3 (%)
GG-S01G	0.006	nd	0.265	5.09	0.75	20.45	nd	73.43	0.010	nd	nd
GG-S02G	0.007	nd	0.051	0.65	0.65	3.20	nd	95.43	0.012	nd	nd
GG-S03G	0.008	nd	0.065	0.46	1.13	3.96	nd	94.36	0.012	nd	nd
GG-S06G	0.008	nd	0.176	0.95	0.43	7.73	nd	90.70	0.009	nd	nd
GG-S09G	0.008	nd	0.060	0.40	0.40	2.87	nd	96.25	0.010	nd	nd

Sample Name	C_3H_6 (%)	iC_4 (%)	nC_4 (%)	iC_5 (%)	nC_5 (%)	C_6+ (%)	MS	$d^{13}C_1$ (‰)	dDC_1 (‰)	Specific Gravity	BTU
GG-S01G	nd	nd	nd	nd	nd	0.000	11/19/2018	-48.85	-273.7	0.676	744
GG-S02G	nd	nd	nd	nd	nd	0.000	11/19/2018	-48.68	-272.2	0.577	968
GG-S03G	nd	nd	nd	nd	nd	nd	11/19/2018	-47.32	-267.9	0.584	957
GG-S06G	nd	nd	nd	nd	nd	nd	11/19/2018	-58.56	-289.3	0.597	920
GG-S09G	nd	nd	nd	nd	nd	nd	11/19/2018	-47.26	-266.1	0.572	976